Annual Reviews in Control 57 (2024) 100944

Contents lists available at ScienceDirect

Annual Reviews in Control

journal homepage: www.elsevier.com/locate/arcontrol

Toward model-free safety-critical control with humans in the loop ☆

Wei Xiao [a,*], Anni Li [b], Christos G. Cassandras [b], Calin Belta [b]

[a] Computer Science and Artificial Intelligence Lab, Massachusetts Institute of Technology, USA
[b] Division of Systems Engineering and Center for Information and Systems Engineering, Boston University, Brookline, MA, 02446, USA

ARTICLE INFO

Keywords:
Unknown dynamics
Event-driven control
Model-free control
Human in the loop

ABSTRACT

This vision article shows how to build on the framework of event-triggered Control Barrier Functions (CBFs) to design model-free controllers for safety-critical multi-agent systems with unknown dynamics, including humans in the loop. This event-triggered framework has been shown to be computationally efficient and robust while guaranteeing safety for systems with unknown dynamics. We show how to extend it to model-free safety critical control where a controllable ego agent does not need to model the dynamics of other agents and updates its control based only on events dependent on the error states of agents obtained by real-time sensor measurements. To facilitate the process of real-time sensor measurements critical in this approach, we also present CBF relative degree reduction methods, which can reduce the number of such measurements. We illustrate the effectiveness of the proposed framework on a multi-agent traffic merging decentralized control problem and on highway lane changing control with humans in the loop and relative degree reduction. We also compare the proposed event-driven method to the classical time-driven approach.

1. Introduction

Safety constrained optimal control problems are central to proliferating safety-critical autonomous and cyber–physical systems. Traditional Hamiltonian analysis (Bryson & Ho, 1969) and dynamic programming (Denardo, 2003) cannot accommodate the size and nonlinearities of such systems, and they only work efficiently for small-scale linear systems. Model Predictive Control (MPC) (Rawlings, Mayne, & Diehl, 2018) methods have been shown to work for large, non-linear systems that can be easily linearized. However, safety requirements are hard to guarantee. Motivated by these limitations, barrier and control barrier functions enforcing hard safety constraints have received increased attention in recent years (Ames, Grizzle, & Tabuada, 2014; Glotfelter, Cortes, & Egerstedt, 2017; Xiao & Belta, 2019; Xiao, Cassandras, & Belta, 2023).

Barrier functions (BFs) (Tee, Ge, & Tay, 2009; Wieland & Allgower, 2007) originate from optimization problems (Boyd & Vandenberghe, 2004) where they are mainly used to enforce constraints in a soft manner (i.e., no guarantees that the constraints are satisfied), and they have been recently employed to prove set invariance (Aubin, 2009), Prajna, Jadbabaie, and Pappas (2007), Wisniewski and Sloth (2013). In particular, it was proved that if a BF for a given set satisfies Lyapunov-like conditions with respect to a system's dynamics, then the set is forward invariant for that system (Tee et al., 2009). Control BFs (CBFs) are extensions of BFs for control systems, and are used to map a constraint defined over system states into a constraint on the control input. In contrast to BFs, CBFs are mainly used to address hard constraints that can strictly enforce safety constraints. In its original form Ames et al. (2014), Glotfelter et al. (2017), the CBF works for constraints that have relative degree one with respect to the system dynamics. The exponential CBF (Nguyen & Sreenath, 2016) and the high order CBF (HOCBF) (Xiao & Belta, 2019) work for systems with arbitrary relative degree constraints.

CBFs are usually based on the assumption that the control system is affine in the control and also the cost is quadratic in the control. Convergence to desired states is achieved by Control Lyapunov Functions (CLFs) (Ames, Galloway, & Grizzle, 2012). The time domain is then usually discretized, and the state and control are assumed to be constant over each discrete time step. The optimal control problem is thus reduced to a (possibly large) sequence of Quadratic Program (QPs), one for each time interval (Galloway, Sreenath, Ames, & Grizzle, 2013) over which the control is kept constant. Most existing works based on this QP approach use a uniform time discretization. One of the challenges is to adapt this process (i.e., determine the next time when a QP needs to be solved) so as to guarantee safety. The work in Yang, Belta, and Tron (2019) proposes an approach based on the Lipschitz constants of the system. The authors of Taylor, Ong, Cortes,

☆ This work was supported in part by NSF under grants IIS-1723995, CPS-1446151, ECCS-1931600, DMS-1664644, CNS-1645681, CNS-2149511, by ARPAE under grant DE-AR0001282.

* Corresponding author.
E-mail addresses: weixy@mit.edu (W. Xiao), anlianni@bu.edu (A. Li), cgc@bu.edu (C.G. Cassandras), cbelta@bu.edu (C. Belta).

https://doi.org/10.1016/j.arcontrol.2024.100944
Received 10 December 2023; Accepted 3 March 2024
Available online 18 March 2024

and Ames (2021) use a procedure inspired from event-triggered control for Lyapunov functions (Tabuada, 2007). In Ong and Cortes (2021), the prescribed performance is used to trigger each control update using CBFs. All these approaches assume that the dynamics are accurately modeled, which is often not the case in reality. To infer dynamics, machine learning techniques can be used (Taylor, Singletary, Yue, & Ames, 2020) Khojasteh, Dhiman, Franceschetti, and Atanasov (2020), which are computationally expensive and not guaranteed to yield sufficiently accurate dynamics for the CBF method. Although it is possible to still guarantee safety through uncertainty bounds (Taylor et al., 2020) or for probabilistic satisfaction (Khojasteh et al., 2020), the conservativeness issue that often arises is difficult to address. The work in Sadraddini and Belta (2018) uses piecewise linear systems to estimate the system dynamics, which is also computationally expensive. Moreover, all these approaches fail to work for systems (such as time-varying systems) that require online model identification. In contrast, we focus on how to address the safety-critical problem with unknown dynamics in an online and less-conservative fashion. CBFs specifically applied to multi-agent systems have also been extensively studied in Borrmann, Wang, Ames, and Egerstedt (2015), Cheng, Khojasteh, Ames, and Burdick (2020). However, when an ego agent must design its own controller, the dynamics of other agents are even harder to identify, an issue that we also address here.

In Xiao, Belta, and Cassandras (2023), we developed a robust framework by defining adaptive affine dynamics that are updated in a time-efficient way to approximate the actual unmodeled dynamics. The adaptive and real dynamics are related through the error states obtained by real-time sensor measurements. We define a HOCBF for a safety requirement on the actual system based on the adaptive dynamics and error states, and reformulate the safety-critical control problem as the above mentioned sequence of QPs. We determine a set of events required to trigger each QP solution in order to ensure safety and derive a condition that guarantees the satisfaction of the HOCBF constraint between events. The triggering of events is based on the value of the HOCBF. The adaptive dynamics are updated at each event to accommodate the real dynamics according to the error states.

Compared to the traditional time-triggered framework (Ames et al., 2014; Glotfelter et al., 2017; Xiao & Belta, 2019), the proposed method can (a) deal with the inter-sampling effect (i.e., the satisfaction of safety constraints within each discretized time interval), (b) This also frees us from the need to select and tune a time step parameter which is a challenging problem, (c) The proposed event-triggered method can significantly reduce the frequency of solving the optimization problem (since the number of triggering events is generally much smaller than the number of discretized time steps), thus we can save computational resources, and (d) We can improve the resilience with respect to cyber-attacks (Ahmad, Sabouni, Xiao, Cassandras, & Li, 2023; Sabouni, Cassandras, Xiao, & Meskin, 2024) in inter-connected control systems (e.g., connected and automated vehicles considered in our paper) in which case system (state) information is shared among different agents. Compared to other event-triggered frameworks (Ong & Cortes, 2021; Tabuada, 2007; Taylor et al., 2021; Yang et al., 2019) that mostly consider single-agent problems, the proposed method can guarantee safety for multi-agent systems with unknown dynamics.

The goal of this vision article is to review a previously proposed event-triggered control method for safe multi-agent systems with unknown dynamics, and use it as the starting point for several further research directions. Specifically, we start by revisiting the event-triggered framework from Xiao, Belta, and Cassandras (2023), which guarantees safety for systems with unknown dynamics. Based on this, the contributions of this article are:

(1) A model-free approach for multi-agent systems, in which the controlled (ego) agent does not need to model the dynamics of the other agents. We show that this can also simplify the formulations of event-triggered CBFs, and discuss a research direction towards a completely dynamics-free, safety-critical control framework (i.e., the identification of the adaptive control-affine dynamics for the ego agent can also be avoided).
(2) We show how we can easily incorporate human actions into the control loop of multi-agent systems based on the proposed framework. This is demonstrated through a safe highway lane changing control problem in a mixed traffic scenario, where both the human driven vehicle dynamics and human control policies are unavailable to the automated vehicles.
(3) Motivated by the need for measurements of high-order derivatives of system states (especially for other agents) in the event-triggered framework, we discuss directions for new research on relative degree reduction, including the need to reduce the conservativeness of this method.

The paper is structured as follows. We present preliminaries on Control Barrier Functions (CBFs) and High Order CBFs in Section 2, and formulate our problem and present a brief summary to the problem solution in Sections 3 and 4, respectively. In Section 5, we first revisit the event-triggered CBFs from Xiao, Belta, and Cassandras (2023), and then propose further solutions and research directions for model-free methods, human-in-the-loop control, and relative degree reduction methods. We present two case studies regarding safe multi-agent control problems (one for traffic merging and one for highway lane change maneuvering with human-in-the-loop) in Section 6, and conclude the paper in Section 7 with future directions.

2. Preliminaries

Definition 1 (*Class $\mathcal{K}$ Function (Khalil, 2002)*)**.** A continuous function $\alpha : [0, a) \to [0, \infty), a > 0$ is said to belong to class $\mathcal{K}$ if it is strictly increasing and $\alpha(0) = 0$.

Consider an affine control system (assumed to be known in this section) of the form

$$\dot{\boldsymbol{x}} = f(\boldsymbol{x}) + g(\boldsymbol{x})\boldsymbol{u} \tag{1}$$

where $\boldsymbol{x} \in X \subset \mathbb{R}^n$, where X is a closed state constraint set, $f : \mathbb{R}^n \to \mathbb{R}^n$ and $g : \mathbb{R}^n \to \mathbb{R}^{n\times q}$ are Lipschitz continuous, and $\boldsymbol{u} \in U \subset \mathbb{R}^q$ is a closed control constraint set defined as

$$U := \{\boldsymbol{u} \in \mathbb{R}^q : \boldsymbol{u}_{min} \le \boldsymbol{u} \le \boldsymbol{u}_{max}\}. \tag{2}$$

with $\boldsymbol{u}_{min}, \boldsymbol{u}_{max} \in \mathbb{R}^q$ and the inequalities are interpreted componentwise.

Definition 2. A set $C \subset \mathbb{R}^n$ is forward invariant for system (1) if its solutions starting at any $\boldsymbol{x}(0) \in C$ satisfy $\boldsymbol{x}(t) \in C$, $\forall t \ge 0$.

Definition 3 (*Relative Degree*)**.** The relative degree of a (sufficiently many times) differentiable function $b : \mathbb{R}^n \to \mathbb{R}$ with respect to system (1) is the number of times it needs to be differentiated along its dynamics until the control $\boldsymbol{u}$ explicitly shows in the corresponding derivative.

Given a function b and a constraint $b(\boldsymbol{x}) \ge 0$, we will also refer to the relative degree of b as the relative degree of the constraint.

For a constraint $b(\boldsymbol{x}) \ge 0$ with relative degree m, $b : \mathbb{R}^n \to \mathbb{R}$, and $\psi_0(\boldsymbol{x}) := b(\boldsymbol{x})$, we define a sequence of functions $\psi_i : \mathbb{R}^n \to \mathbb{R}, i \in \{1, \dots, m\}$:

$$\psi_i(\boldsymbol{x}) := \dot{\psi}_{i-1}(\boldsymbol{x}) + \alpha_i(\psi_{i-1}(\boldsymbol{x})), i \in \{1, \dots, m\}, \tag{3}$$

where $\alpha_i(\cdot)$, $i \in \{1, \dots, m\}$, denotes a $(m - i)^{th}$ order differentiable class $\mathcal{K}$ function.

We further define a sequence of sets C_i, $i \in \{1, \dots, m\}$, associated with (3) in the form:

$$C_i := \{\boldsymbol{x} \in X : \psi_{i-1}(\boldsymbol{x}) \ge 0\}, i \in \{1, \dots, m\}. \tag{4}$$

Definition 4 (*High Order Control Barrier Function (HOCBF) (Xiao & Belta, 2019)*)**.** Let $C_1, \dots, C_m$ be defined by (4) and $\psi_1(\boldsymbol{x}), \dots, \psi_m(\boldsymbol{x})$ be defined by (3). A function $b : \mathbb{R}^n \to \mathbb{R}$ is a High Order Control Barrier Function (HOCBF) of relative degree m for system (1) if there exist $(m-i)^{th}$ order differentiable class $\mathcal{K}$ functions $\alpha_i, i \in \{1, \dots, m-1\}$ and a class $\mathcal{K}$ function α_m such that

$$\sup_{\boldsymbol{u} \in U} [L_f^m b(\boldsymbol{x}) + L_g L_f^{m-1} b(\boldsymbol{x})\boldsymbol{u} + R(b(\boldsymbol{x})) + \alpha_m(\psi_{m-1}(\boldsymbol{x}))] \geq 0, \tag{5}$$

for all $\boldsymbol{x} \in C_1 \cap, \dots, \cap C_m$. In (5), L_f^m (L_g) denotes Lie derivatives along f (g) m (one) times, and $R(\cdot)$ denotes the remaining Lie derivatives along f with degree less than or equal to $m-1$ (omitted for simplicity, see Xiao and Belta (2019)). Moreover, it is assumed that $L_g L_f^{m-1} b(\boldsymbol{x}) \neq 0$ when $b(\boldsymbol{x}) = 0$.

The HOCBF is a general form of the relative degree one CBF (Ames et al., 2014; Glotfelter et al., 2017), Lindemann and Dimarogonas (2019), i.e., setting $m = 1$ reduces the HOCBF to the common CBF form (it is assumed that $L_g b(\boldsymbol{x}) \neq 0$ when $b(\boldsymbol{x}) = 0$):

$$L_f b(\boldsymbol{x}) + L_g b(\boldsymbol{x})\boldsymbol{u} + \alpha_1(b(\boldsymbol{x})) \geq 0, \tag{6}$$

and it is also a general form of the exponential CBF (Nguyen & Sreenath, 2016).

Theorem 1 (*Xiao and Belta (2019)*)**.** *Given a HOCBF $b(\boldsymbol{x})$ from Definition 4 with the associated sets $C_1, \dots, C_m$ defined by (4), if $\boldsymbol{x}(0) \in C_1 \cap, \dots, \cap C_m$, then any Lipschitz continuous controller $\boldsymbol{u}(t)$ that satisfies (5), $\forall t \geq 0$ renders $C_1 \cap, \dots, \cap C_m$ forward invariant for system (1).*

Definition 5 (*Control Lyapunov Function (CLF) (Ames et al., 2012)*)**.** A continuously differentiable function $V : \mathbb{R}^n \to \mathbb{R}$ is an exponentially stabilizing control Lyapunov function (CLF) for system (1) if there exist constants $c_1 > 0, c_2 > 0, c_3 > 0$ such that for $\forall \boldsymbol{x} \in \mathbb{R}^n$, $c_1 \|\boldsymbol{x}\|^2 \leq V(\boldsymbol{x}) \leq c_2 \|\boldsymbol{x}\|^2$,

$$\inf_{\boldsymbol{u} \in U} [L_f V(\boldsymbol{x}) + L_g V(\boldsymbol{x})\boldsymbol{u} + c_3 V(\boldsymbol{x})] \leq 0. \tag{7}$$

Many existing works (Ames et al., 2014), Nguyen and Sreenath (2016), Yang et al. (2019) combine CBFs for systems with relative degree one with quadratic costs to form optimization problems. An explicit solution to such problems can be obtained based on some assumptions (Ames, Xu, Grizzle, & Tabuada, 2017). Alternatively, we can discretize time and an optimization problem with constraints given by the CBFs (inequalities of the form (5)) is solved at each time step. The inter-sampling effect in this approach is considered in Yang et al. (2019). If convergence to a state is desired, then a CLF constraint of the form (7) is added, as in Ames et al. (2014) (Yang et al., 2019). Note that these constraints are linear in the control since the state value is fixed at the beginning of the interval. Therefore, each optimization problem is a quadratic program (QP). The optimal control obtained by solving each QP is applied at the current time step and held constant for the whole interval. The state is updated using dynamics (1), and the procedure is repeated. Replacing CBFs by HOCBFs allows us to handle constraints with arbitrary relative degree (Xiao & Belta, 2019). Throughout the paper, we will refer to this method as the *time-driven* approach. The CBF method works if (1) is an accurate model for the system. However, this is often not the case in reality, especially for time-varying systems. In what follows, we show how we can find a safety-guaranteed controller for systems with unknown dynamics.

3. Problem formulation

We consider a multi-agent system with a controlled agent (state $\boldsymbol{x} \in X$ and control $\boldsymbol{u} \in U$) whose dynamics are unknown, and with a set S_a of other agents (state $\boldsymbol{y}_i \in X$ for agent $i \in S_a$) whose dynamics are also unknown. For instance, the controlled agent could be the ego vehicle in autonomous driving, and the other agents are either other vehicles or obstacles. The controlled agent only has onboard sensors to detect its own state and that of other agents (which may be controlled by humans). We make the following assumption about the unknown dynamics of both controlled and uncontrolled agents:

Assumption 1. The relative degree of each component of $\boldsymbol{x}$ with respect to the real unknown dynamics[1] is known for the real unknown dynamics, and the same applies to $\boldsymbol{y}_i, i \in S_a$.

A typical example for the above assumption is the autonomous driving problem, in which case we have a controlled (ego) vehicle and some other vehicles around the controlled one. If the position of the controlled vehicle (whose dynamics are unknown) is a component in $\boldsymbol{x}$ and the control is acceleration, then the relative degree of the position with respect to the unknown vehicle dynamics is two by Newton's law. The same applies to other vehicles that the controlled vehicle may interact with. We assume that we have sensors to monitor $\boldsymbol{x}$ and its derivatives, as well as to monitor $\boldsymbol{y}_i$ and its derivatives for all $i \in S_a$. Measuring derivatives of $\boldsymbol{x}$ can be challenging, but accurate measurements may not be necessary: in fact, we can relax this requirement by limiting measurement accuracy within some bounds, as shown later.

Objective 1 (*Minimizing Cost*)**.** Consider an optimal control problem for the real unknown dynamics of the controlled agent with the cost:

$$\min_{\boldsymbol{u}(t)} \int_0^T C(\|\boldsymbol{u}(t)\|) dt \tag{8}$$

where $\|\cdot\|$ denotes the 2-norm of a vector, $C(\cdot)$ is a strictly increasing function of its argument. $T > 0$.

Objective 2 (*Terminal State Constraint*)**.** We wish the terminal state $\boldsymbol{x}(T)$ to reach a point $\boldsymbol{K}$, where $\boldsymbol{K} \in \mathbb{R}^n$.

Objective 2 can be easily extended to multiple terminal state constraints for different desired points.

Safety requirements: The real unknown dynamics of the controlled agent should always satisfy a safety requirement with respect to another agent $i \in S_a$ whose dynamics are also unknown:

$$b(\boldsymbol{x}(t), \boldsymbol{y}_i(t)) \geq 0, \forall t \in [0, T], \tag{9}$$

where $b : \mathbb{R}^n \times \mathbb{R}^n \to \mathbb{R}$ is continuously differentiable and has relative degree $m \in \mathbb{N}$ with respect to the real dynamics of the controlled agent.

The above safety constraint is defined pairwise, but can be extended to involve more than two agents. The relative degree m is known by Assumption 1.

Control constraints: The controlled agent should always satisfy control bounds in the form of (2).

A control policy for the real unknown dynamics of the controlled agent is ***feasible*** if constraints (2) and (9) are satisfied at all times. Note that state limitations are particular forms of (9) that only depend on the state $\boldsymbol{x}$. In this paper, we consider the following problem:

Problem 1. Given real-time sensor measurements for $\boldsymbol{x}, \boldsymbol{y}_i, i \in S_a$ and their derivatives, find an online and feasible control policy for the real unknown dynamics of the controlled agent such that the cost (8) is minimized.

The above optimal control problem is assumed to be feasible. Due to the unknown dynamics, the problem is generally hard to solve using optimal control methods such as Hamiltonian analysis. One way to address this is to assume linear models for all agents, which often

[1] The derivative of each component of $\boldsymbol{x}$ is a function of the whole state $\boldsymbol{x}$ according to the dynamics of the system. The relative degree can then we defined using Definition 3

allows us to find analytical optimal controls for all the agents, as shown in Xiao and Cassandras (2021). Then, we may use the optimal solutions as a reference for the low level controllers, such as the CBF-based QP controller, that accounts for the system unknown dynamics. Optimal control solutions and case studies can be found in Xiao and Cassandras (2021). In this paper, we focus on the safety of multi-agent systems with unknown dynamics. We first review solutions using the event-triggered CBFs (Xiao, Belta, & Cassandras, 2023), as shown in the next section, and then discuss new approaches regarding model-free methods, relative degree reduction, and a human in the loop study for real world applications.

4. Approach

In order to solve Problem 1 in an online fashion, we replace the safety constraints above by HOCBF constraints, and solve it through a sequence of discretization steps. Thus, Problem 1 is solved by pointwise optimization, which leads to sub-optimal solutions compared to the original problem. As detailed in Xiao, Belta, and Cassandras (2023), there are four steps involved in the solution:

Step 1: define adaptive affine dynamics for the controlled agent and adaptive dynamics for other agents. We need affine dynamics of the form (1) in order to apply the CBF-based QP approach to solve Problem 1. Under Assumption 1, we define affine dynamics that have the same relative degree for (9) as the real controlled agent and we estimate through $\bar{\boldsymbol{x}}$ the actual state $\boldsymbol{x}$ using the dynamics:

$$\dot{\bar{\boldsymbol{x}}} = f_a(\bar{\boldsymbol{x}}) + g_a(\bar{\boldsymbol{x}})\boldsymbol{u} \tag{10}$$

where $f_a : \mathbb{R}^n \to \mathbb{R}, g_a : \mathbb{R}^n \to \mathbb{R}^{n\times q}$, and $\bar{\boldsymbol{x}} \in X \subset \mathbb{R}^n$ is the state vector corresponding to $\boldsymbol{x}$ in the unknown dynamics. Since $f_a(\cdot), g_a(\cdot)$ in (10) can be adaptively updated to accommodate the real unknown dynamics, as shown in the next section, we call (10) *adaptive affine dynamics*. The real unknown dynamics and (10) are related through the error states $\boldsymbol{e} := \boldsymbol{x} - \bar{\boldsymbol{x}}$ obtained from the real-time measurements of the agent and the integration of (10) as f_a, g_a are known. Based on user-defined bounds for these errors, the convergence of the adaptive affine dynamics (10) to the real dynamics depends on the update events. Theoretically, we can consider any affine dynamics in (10) to model the agent as long as their states are of the same dimension and with the same physical interpretation as those of the plant. Clearly, we would like the adaptive dynamics (10) to "stay close" to the real dynamics. This notion will be formalized in the next section.

Along the same lines, if other agents have their own (unknown) dynamic models, we also define adaptive dynamics for each agent $i \in S_a$ to estimate its real unknown dynamics in the form:

$$\dot{\bar{\boldsymbol{y}}}_i = h_{a,i}(\bar{\boldsymbol{y}}_i) \tag{11}$$

where $\bar{\boldsymbol{y}}_i \in X$ with $h_{a,i} : \mathbb{R}^n \to \mathbb{R}$, and $\bar{\boldsymbol{y}}_i$ is the state vector corresponding to $\boldsymbol{y}_i$ in the unknown dynamics. Note that $h_{a,i}(\cdot)$ will also be adaptively updated and we refer to (11) as *adaptive dynamics*. The real unknown dynamics of agent $i \in S_o$ and (11) are also related through the error states obtained from the real-time measurements of the agent and the integration of (11) (as $h_{a,i}$ is known). Observe that it is possible that $h_{a,i}(\cdot)$ also includes the control of agent i (which is omitted for simplicity), in which case we have a multi-agent control problem. We may define adaptive affine dynamics as in (10) for other agents as well. Our approach in this paper can also work for such multi-agent control problems (in which case (11) is also affine in control). We can also explicitly model the human controlled agents similarly, in which case we may predict the human control and study human-autonomous system interactions. We focus only on decentralized multi-agent control problems in this paper for simplicity, but the proposed framework can be applied to cases in which controls should be jointly determined (as in game theory). Therefore, we omit the control component in $h_{a,i}(\cdot)$.

Model-free cases. Unlike the analysis in Xiao, Belta, and Cassandras (2023), we do not wish to find controls for other agents and to avoid the estimation of the adaptive dynamics (11). Thus, we may directly use $\boldsymbol{y}_i$ and its derivatives in formulating CBFs/HOCBFs. This is what we refer to as *model-free safety-critical control* in this paper.

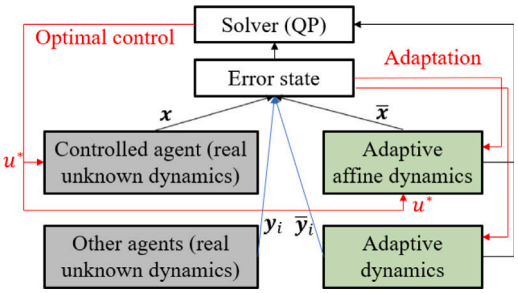

Fig. 1. The solution framework for Problem 1 using adaptive dynamics for all agents (joint optimal control for multi-agent systems is possible), the connection between the real unknown dynamics of the controlled agent and the adaptive affine dynamics (10), and the connection between the real unknown dynamics of other agents in S_a and the adaptive dynamics (11). The states $\boldsymbol{x}, \boldsymbol{y}_i, i \in S_a$ are from the sensor measurements of the controlled agent and the other agents.

Step 2: find a HOCBF that guarantees (9). Based on (10), (11) (or, directly, $\boldsymbol{y}_i$ and its derivatives), the error state and its derivatives, we use a HOCBF to enforce (9). Details are shown in the next section.

Step 3: formulate the CBF-based QP. We use a CLF to have the terminal state approach $\boldsymbol{K}$ in Objective 2. The approach to guarantee convergence for unknown dynamics is similar to the above mentioned HOCBF method, and it will be presented in the following sections. If $C(\|\boldsymbol{u}(t)\|) = \|\boldsymbol{u}(t)\|^2$ in (8), then we can formulate Problem 1 using a CBF-CLF-QP approach (Ames et al., 2014), with a CBF replaced by a HOCBF (Xiao & Belta, 2019) if $m > 1$.

Step 4: determine the events required to specify when to solve the QP and the conditions that guarantee the satisfaction of (9) **between events.** We need to determine the event times $t_k, k = 1, 2, \ldots (t_1 = 0)$ at which each QP must be solved in order to guarantee the satisfaction of (9) for the real unknown dynamics. Since there is obviously a difference between the adaptive affine dynamics (10) and the real unknown dynamics of the controlled agent (as well as between the adaptive dynamics (11) and other agents), in order to guarantee safety for the controlled agent, we need to properly define events (dependent on the error states, the state of (10), and the state of (11) or $\boldsymbol{y}_i$ and its derivatives in model-free cases) to solve the QP.

The proposed solution framework is outlined in Fig. 1 (from Xiao, Belta, and Cassandras (2023)) with the extension to model-free cases for all other agents shown in Fig. 2, where we note that we apply the same control from the QP to both the real unknown dynamics of the controlled agent and to the adaptive affine dynamics in (10). We also point out that in a static environment, i.e., other agent states do not change or are known, we can remove the adaptive dynamics and other plant blocks in Figs. 1 and 2.

5. Safety-critical control

In this section, we treat the terminal cost in Objective 2 as a soft constraint, and provide the technical details involved in formulating the CBF-based QPs that guarantee the satisfaction of the safety constraint (9) for the controlled agent. We start with a review from Xiao, Belta, and Cassandras (2023) of the case that includes adaptive dynamics for all the agents in multi-agent systems and then present the extension to the model-free case.

5.1. Model-based methods for unknown dynamics

In this subsection, we review the event-triggered CBF method (Xiao, Belta, & Cassandras, 2023) to motivate new directions along this line.

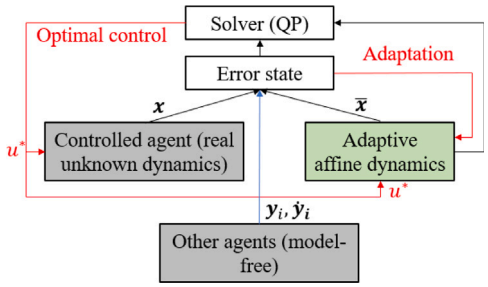

Fig. 2. The solution framework for Problem 1 in which case all other agents are model-free (only decentralized optimal control for the ego agent is possible), the connection between the real unknown dynamics of the controlled agent and the adaptive affine dynamics (10). The states $\boldsymbol{x}, \boldsymbol{y}_i, \dot{\boldsymbol{y}}_i, i \in S_a$ are from the sensor measurements of the controlled agent and the other agents.

We first consider the case that the safety constraint in (9) has relative degree one with respect to both dynamics (10) and the actual dynamics of the controlled agent. In this case, since (9) involves the state of both the controlled agent and agent $i \in S_a$, the set C_1 corresponding to (4) takes the form:

$$C_1 = \{(\boldsymbol{x}, \boldsymbol{y}_i) \in X \times X : b(\boldsymbol{x}, \boldsymbol{y}_i) \geq 0\}. \tag{12}$$

Next, we show how to find a CBF that guarantees (9) for the real unknown dynamics. Let

$$\boldsymbol{e}_x := \boldsymbol{x} - \bar{\boldsymbol{x}}, \qquad \boldsymbol{e}_i = \boldsymbol{y}_i - \bar{\boldsymbol{y}}_i, i \in S_a. \tag{13}$$

Note that $\boldsymbol{x}$ and $\bar{\boldsymbol{x}}$ are state vectors from direct measurements of the controlled agent and from the adaptive affine dynamics (10), respectively, and $\boldsymbol{y}_i$ and $\bar{\boldsymbol{y}}_i$ are state vectors from direct measurements of agent $i \in S_a$ and from the adaptive dynamics (11), respectively. Then,

$$b(\boldsymbol{x}, \boldsymbol{y}_i) = b(\bar{\boldsymbol{x}} + \boldsymbol{e}_x, \bar{\boldsymbol{y}}_i + \boldsymbol{e}_i). \tag{14}$$

Differentiating $b(\bar{\boldsymbol{x}} + \boldsymbol{e}_x, \bar{\boldsymbol{y}}_i + \boldsymbol{e}_i)$, we have

$$\begin{aligned}\frac{db(\bar{\boldsymbol{x}}+\boldsymbol{e}_x, \bar{\boldsymbol{y}}_i+\boldsymbol{e}_i)}{dt} = &\frac{\partial b(\bar{\boldsymbol{x}}+\boldsymbol{e}_x, \bar{\boldsymbol{y}}_i+\boldsymbol{e}_i)}{\partial \bar{\boldsymbol{x}}}\dot{\bar{\boldsymbol{x}}} + \frac{\partial b(\bar{\boldsymbol{x}}+\boldsymbol{e}_x, \bar{\boldsymbol{y}}_i+\boldsymbol{e}_i)}{\partial \boldsymbol{e}_x}\dot{\boldsymbol{e}}_x \\ &+ \frac{\partial b(\bar{\boldsymbol{x}}+\boldsymbol{e}_x, \bar{\boldsymbol{y}}_i+\boldsymbol{e}_i)}{\partial \bar{\boldsymbol{y}}_i}\dot{\bar{\boldsymbol{y}}}_i + \frac{\partial b(\bar{\boldsymbol{x}}+\boldsymbol{e}_x, \bar{\boldsymbol{y}}_i+\boldsymbol{e}_i)}{\partial \boldsymbol{e}_i}\dot{\boldsymbol{e}}_i\end{aligned} \tag{15}$$

where $\dot{\boldsymbol{e}}_x = \dot{\boldsymbol{x}} - \dot{\bar{\boldsymbol{x}}}, \dot{\boldsymbol{e}}_i = \dot{\boldsymbol{y}}_i - \dot{\bar{\boldsymbol{y}}}_i$ are evaluated online through $\dot{\boldsymbol{x}}$, $\dot{\boldsymbol{y}}_i$ (from direct measurements of the actual state derivatives) and $\dot{\bar{\boldsymbol{x}}}, \dot{\bar{\boldsymbol{y}}}_i$ are given through (10), (11), respectively. Note that $\dot{\bar{\boldsymbol{x}}}$ would be involved with the control $\boldsymbol{u}$ due to the adaptive affine dynamics (10) and the fact that the safety constraint has relative degree one. The same applies to $\dot{\bar{\boldsymbol{y}}}_i$. This formulation allows us to get a control constraint over the ego agent and/or agent $i \in S_a$.

Remark 1 (*Measurement Uncertainties*)**.** If the measurements $\boldsymbol{x}$ and $\dot{\boldsymbol{x}}$ (or $\boldsymbol{y}_i$ and $\dot{\boldsymbol{y}}_i$) are subject to uncertainties, and the uncertainties are bounded, then we can apply the bounds of $\boldsymbol{x}$ and $\dot{\boldsymbol{x}}$ (or $\boldsymbol{y}_i$ and $\dot{\boldsymbol{y}}_i$) in evaluating the next event time t_{k+1} (introduced later) instead of $\boldsymbol{x}$ and $\dot{\boldsymbol{x}}$ (or $\boldsymbol{y}_i$ and $\dot{\boldsymbol{y}}_i$) themselves. In other words, $\boldsymbol{e}_x(t)$ and $\dot{\boldsymbol{e}}_x(t)$ ($\boldsymbol{e}_i(t)$ and $\dot{\boldsymbol{e}}_i(t)$) are determined by the bounds of $\boldsymbol{x}$, $\dot{\boldsymbol{x}}$ (or $\boldsymbol{y}_i$ and $\dot{\boldsymbol{y}}_i$) and the state values of the adaptive affine system (10) (or (11)).

The CBF constraint that guarantees (9) for known dynamics (1) is as in (6), which is obtained by replacing $\dot{\boldsymbol{x}}$ with (1). However, for the unknown dynamics, the CBF constraint is:

$$\frac{db(\boldsymbol{x}, \boldsymbol{y}_i)}{dt} + \alpha_1(b(\boldsymbol{x}, \boldsymbol{y}_i)) \geq 0.$$

Equivalently, we have

$$\frac{db(\bar{\boldsymbol{x}}+\boldsymbol{e}_x, \bar{\boldsymbol{y}}_i+\boldsymbol{e}_i)}{dt} + \alpha_1(b(\bar{\boldsymbol{x}}+\boldsymbol{e}_x, \bar{\boldsymbol{y}}_i+\boldsymbol{e}_i)) \geq 0. \tag{16}$$

Combining (15), (16), (10) and (11), we get the CBF constraint that guarantees (9):

$$\begin{aligned}&\frac{\partial b(\boldsymbol{x}, \boldsymbol{y}_i)}{\partial \bar{\boldsymbol{x}}} f_a(\bar{\boldsymbol{x}}) + \frac{\partial b(\boldsymbol{x}, \boldsymbol{y}_i)}{\partial \bar{\boldsymbol{x}}} g_a(\bar{\boldsymbol{x}})\boldsymbol{u} + \frac{\partial b(\boldsymbol{x}, \boldsymbol{y}_i)}{\partial \boldsymbol{e}_x}\dot{\boldsymbol{e}}_x \\ &+ \frac{\partial b(\boldsymbol{x}, \boldsymbol{y}_i)}{\partial \bar{\boldsymbol{y}}_i} h_{a,i}(\bar{\boldsymbol{y}}_i) + \frac{\partial b(\boldsymbol{x}, \boldsymbol{y}_i)}{\partial \boldsymbol{e}_i}\dot{\boldsymbol{e}}_i + \alpha_1(b(\boldsymbol{x}, \boldsymbol{y}_i)) \geq 0.\end{aligned} \tag{17}$$

Recall that we may have the control input showing up in $h_{a,i}(\bar{\boldsymbol{y}}_i)$, in which case the above CBF constraint (17) depends on both the control input $\boldsymbol{u}$ of the current controlled agent and the control $\boldsymbol{u}_i$ of agent $i \in S_a$. In other words, we have a multi-agent control problem that jointly determines all control inputs for safety guarantees, which can still be obtained using the proposed framework. The above constraint can also build safe human interaction when there are some human-controlled agents since both human control and the control of autonomous agent will show up in (17). Then, the satisfaction of (17) implies the satisfaction of $b(\bar{\boldsymbol{x}} + \boldsymbol{e}_x, \bar{\boldsymbol{y}}_i + \boldsymbol{e}_i) \geq 0$ by Theorem 1 and (14). Thus, (9) is guaranteed to be satisfied for the real unknown dynamics of the controlled agent. For the above CBF constraint, we have the following assumption:

Assumption 2. $\frac{\partial b(\boldsymbol{x}, \boldsymbol{y}_i)}{\partial \bar{\boldsymbol{x}}} g_a(\bar{\boldsymbol{x}}) \neq \boldsymbol{0}, \forall \boldsymbol{x} \in X, \forall \boldsymbol{y}_i \in X$ such that $b(\boldsymbol{x}, \boldsymbol{y}_i) = 0$.

This assumption may not be necessary for a safety-enforcing CBF, as the system trajectory with a CBF (HOCBF) for safety will never reach the safe set boundary, as shown in Lemma 1 of Xiao, Belta, and Cassandras (2021b), if we define power class-$\mathcal{K}$ functions with power no less than 1 in the CBF and if the initial state is inside the safe set. If Assumption 2 does not hold and the CBF constraint (17) is not satisfied (without the $\boldsymbol{u}$ component) at the boundary of the set C_1, then we may shrink the safe set (if the manifold of $\{(\boldsymbol{x}, \boldsymbol{y}_i) | \frac{\partial b}{\partial \boldsymbol{x}} = 0\}$ does not cut through the safe set) or define another CBF so that the system avoids those states (Tan, Shaw Cortez, & Dimarogonas, 2021); however, this approach can make the system conservative. We may also define a higher relative degree CBF than needed so as to address this problem. A more general non-conservative approach is the subject of future research.

Note that, if $\boldsymbol{y}_i$ in (9) and the dynamics (11) are known, we may just consider a single agent control problem, i.e. we just have $b(\boldsymbol{x})$ instead of $b(\boldsymbol{x}, \boldsymbol{y}_i)$, then we obtain the following simple version of the above CBF constraint:

$$\frac{\partial b(\boldsymbol{x})}{\partial \bar{\boldsymbol{x}}} f_a(\bar{\boldsymbol{x}}) + \frac{\partial b(\boldsymbol{x})}{\partial \bar{\boldsymbol{x}}} g_a(\bar{\boldsymbol{x}})\boldsymbol{u} + \frac{\partial b(\boldsymbol{x})}{\partial \boldsymbol{e}_x}\dot{\boldsymbol{e}}_x + \alpha_1(b(\boldsymbol{x})) \geq 0. \tag{18}$$

Now, we can formulate a CBF-based optimal control problem in the form:

$$\min_{\boldsymbol{u}(t), \delta(t)} \int_0^T \left(\|\boldsymbol{u}(t)\|^2 + p\delta^2(t)\right) dt \tag{19}$$

subject to (17), (2), and the relaxed CLF constraint

$$L_{f_a} V(\bar{\boldsymbol{x}}) + L_{g_a} V(\bar{\boldsymbol{x}})\boldsymbol{u} + \epsilon V(\bar{\boldsymbol{x}}) \leq \delta(t), \tag{20}$$

where $V(\bar{\boldsymbol{x}}) = (\bar{\boldsymbol{x}} - \boldsymbol{K})^T P(\bar{\boldsymbol{x}} - \boldsymbol{K})$, P is positive definite, $c_3 = \epsilon > 0$ in Definition 5, $p > 0$, and $\delta(t)$ is a relaxation for the CLF constraint. Since state convergence is relaxed in this section, we just replace $\boldsymbol{x}$ by $\bar{\boldsymbol{x}}$ in the above CLF constraint. The above optimization is a suboptimal solution of Problem 1 where we assume a quadratic cost corresponding to (8). The use of the relaxation variable $\delta(t)$ is to ensure the problem is always feasible when the state convergence conflicts with safety constraints. In the case of multi-agent control, the above optimization process also allows human-autonomous system interaction that ensures the safety of all agents since both the human control and the control of autonomous agents show up in the CBF constraint (17). Details of this direction are left for future research exploration.

Following the time-driven approach introduced at the end of Section 2, we solve the problem (19) at each time $t_k, k = 1, 2 \ldots$ for a fixed control over the ensuing time step $(t_k, t_{k+1}]$, which therefore

becomes a QP. However, at time t_k, the QP does not generally know the error states $\boldsymbol{e}_x(t), \boldsymbol{e}_i(t)$ and their derivatives $\dot{\boldsymbol{e}}_x(t), \dot{\boldsymbol{e}}_i(t), \forall t > t_k$. Thus, it cannot guarantee that the CBF constraint (17) is satisfied in the time interval $(t_k, t_{k+1}]$, where t_{k+1} is the next time instant to solve the QP. This is what motivates the introduction of *events* defining the conditions needed to guarantee the satisfaction of (17)$\forall t \in (t_k, t_{k+1}]$. We start by imposing bounds on $\boldsymbol{e}_x = (e_{x,1}, \dots, e_{x,n})$ and $\dot{\boldsymbol{e}}_x = (\dot{e}_{x,1}, \dots, \dot{e}_{x,n})$ defined as $\boldsymbol{w} = (w_1, \dots, w_n) \in \mathbb{R}^n_{>0}$ and $\boldsymbol{\nu} = (\nu_1, \dots, \nu_n) \in \mathbb{R}^n_{>0}$:

$$|e_{x,j}| \le w_j, \qquad |\dot{e}_{x,j}| \le \nu_j, \qquad j \in \{1, \dots, n\}. \tag{21}$$

These two inequalities can be rewritten in the form $|\boldsymbol{e}_x| \le \boldsymbol{w}, |\dot{\boldsymbol{e}}_x| \le \boldsymbol{\nu}$ for simplicity. Similarly, we also bound $\boldsymbol{e}_i, \dot{\boldsymbol{e}}_i$:

$$|\boldsymbol{e}_i| \le \boldsymbol{W}_i, \qquad |\dot{\boldsymbol{e}}_i| \le \boldsymbol{V}_i, \qquad i \in S_a. \tag{22}$$

where the inequalities are interpreted componentwise, and $\boldsymbol{W}_i \in \mathbb{R}^n_{>0}, \boldsymbol{V}_i \in \mathbb{R}^n_{>0}$.

Similar to the bounds we introduced for the error states and their derivatives, we also define the following bounds on the deviations of states from their values $\bar{\boldsymbol{x}}(t_k)$ and $\bar{\boldsymbol{y}}_i(t_k), i \in S_a$:

$$\begin{aligned} &\bar{\boldsymbol{x}}(t_k) - \boldsymbol{s}(\beta_1(b(\boldsymbol{x}, \boldsymbol{y}_i))) \le \bar{\boldsymbol{x}} \le \bar{\boldsymbol{x}}(t_k) + \boldsymbol{s}(\beta_1(b(\boldsymbol{x}, \boldsymbol{y}_i))), \\ &\bar{\boldsymbol{y}}_i(t_k) - \boldsymbol{S}_i(\beta_2(b(\boldsymbol{x}, \boldsymbol{y}_i))) \le \bar{\boldsymbol{y}}_i \le \bar{\boldsymbol{y}}_i(t_k) + \boldsymbol{S}_i(\beta_2(b(\boldsymbol{x}, \boldsymbol{y}_i))), \end{aligned} \tag{23}$$

where the inequalities are interpreted componentwise, $\boldsymbol{s} : \mathbb{R} \to \mathbb{R}^n_{>0}, \boldsymbol{S}_i : \mathbb{R} \to \mathbb{R}^n_{>0}$, and $\beta_1(\cdot), \beta_2(\cdot)$ are class $\mathcal{K}$ functions. Proper selection of the above adaptive bounds that depend on the value of CBFs can address the conservativeness of the event-triggered framework, as shown in Xiao, Belta, and Cassandras (2023). For simplicity, we can just use constant vectors $\boldsymbol{s} \in \mathbb{R}^n, \boldsymbol{S}_i \in \mathbb{R}^n$ in the above. Their relative advantages and the choice of $\boldsymbol{s}(\cdot), \boldsymbol{S}_i(\cdot)$ will be discussed later. We denote the set of states that satisfy (23) at time t_k by

$$\begin{aligned} S_x(t_k) = \{\boldsymbol{y}_1 \in X : \bar{\boldsymbol{x}}(t_k) - \boldsymbol{s}(\beta_1(b(\boldsymbol{x}(t_k), \boldsymbol{y}_i(t_k)))) \le \\ \boldsymbol{y}_1 \le \bar{\boldsymbol{x}}(t_k) + \boldsymbol{s}(\beta_1(b(\boldsymbol{x}(t_k), \boldsymbol{y}_i(t_k)))), i \in S_a\}. \end{aligned} \tag{24}$$

$$\begin{aligned} S_{y,i}(t_k) = \{\boldsymbol{y}_2 \in \mathbb{R}^n : \bar{\boldsymbol{y}}_i(t_k) - \boldsymbol{S}_i(\beta_2(b(\boldsymbol{x}(t_k), \boldsymbol{y}_i(t_k)))) \le \\ \boldsymbol{y}_2 \le \bar{\boldsymbol{y}}_i(t_k) + \boldsymbol{S}_i(\beta_2(b(\boldsymbol{x}(t_k), \boldsymbol{y}_i(t_k))))\}. \end{aligned} \tag{25}$$

Now, with (21), (22) and (23), we are ready to find a condition that guarantees the satisfaction of (17) in the time interval $(t_k, t_{k+1}]$. This is done by considering the minimum value of each component in (17), as shown next.

Let $\boldsymbol{z} := (\boldsymbol{y}_1, \boldsymbol{e}_x, \dot{\boldsymbol{e}}_x, \boldsymbol{y}_2, \boldsymbol{e}_i, \dot{\boldsymbol{e}}_i)$, where $\boldsymbol{y}_1 \in S_x(t_k), \boldsymbol{y}_2 \in S_{y,i}(t_k)$. We then define an overall set $S(t_k)$:

$$\begin{aligned} S(t_k) = \{\boldsymbol{z} \in \mathbb{R}^{6n} : \boldsymbol{y}_1 \in S_x(t_k), |\boldsymbol{e}_x| \le \boldsymbol{w}, \\ |\dot{\boldsymbol{e}}_x| \le \boldsymbol{\nu}, \boldsymbol{y}_2 \in S_{y,i}(t_k), |\boldsymbol{e}_i| \le \boldsymbol{W}_i, \\ |\dot{\boldsymbol{e}}_i| \le \boldsymbol{V}_i, (\boldsymbol{y}_1 + \boldsymbol{e}_x, \boldsymbol{y}_2 + \boldsymbol{e}_i) \in C_1, i \in S_a\}. \end{aligned} \tag{26}$$

Consider the first term in (17) and let $b_{f_a,min}(t_k) \in \mathbb{R}$ be the minimum value of $\frac{\partial b(\bar{\boldsymbol{x}}+\boldsymbol{e}_x, \bar{\boldsymbol{y}}_i+\boldsymbol{e}_i)}{\partial \bar{\boldsymbol{x}}} f_a(\bar{\boldsymbol{x}})$ for the preceding time interval that satisfies $\boldsymbol{z} \in S(t_k)$ starting at time t_k, i.e., let

$$b_{f_a,min}(t_k) = \min_{\boldsymbol{z} \in S(t_k)} \frac{\partial b(\boldsymbol{y}_1 + \boldsymbol{e}_x, \boldsymbol{y}_2 + \boldsymbol{e}_i)}{\partial \boldsymbol{y}_1} f_a(\boldsymbol{y}_1). \tag{27}$$

Similarly, we can also find the four scalar minimum values $b_{\alpha_1,min}(t_k)$, $b_{e,min}(t_k)$, $b_{h_{a,i},min}(t_k)$, and $b_{E_i,min}(t_k)$ of $\alpha_1(b(\boldsymbol{x}, \boldsymbol{y}_i))$, $\frac{\partial b(\boldsymbol{x}, \boldsymbol{y}_i)}{\partial \boldsymbol{e}_x} \dot{\boldsymbol{e}}_x$, $\frac{\partial b(\boldsymbol{x}, \boldsymbol{y}_i)}{\partial \bar{\boldsymbol{y}}_i} h_{a,i}(\bar{\boldsymbol{y}}_i)$, $\frac{\partial b(\boldsymbol{x}, \boldsymbol{y}_i)}{\partial \boldsymbol{e}_i} \dot{\boldsymbol{e}}_i, i \in S_a$, respectively, for the preceding time interval $[t_k, t_{k+1}]$ that satisfy $\boldsymbol{z} \in S(t_k)$ starting at time t_k, i.e., let

$$b_{\alpha_1,min}(t_k) = \min_{\boldsymbol{z} \in S(t_k)} \alpha_1(b(\boldsymbol{y}_1 + \boldsymbol{e}_x, \boldsymbol{y}_2 + \boldsymbol{e}_i)), \tag{28}$$

$$b_{e,min}(t_k) = \min_{\boldsymbol{z} \in S(t_k)} \frac{\partial b(\boldsymbol{y}_1 + \boldsymbol{e}_x, \boldsymbol{y}_2 + \boldsymbol{e}_i)}{\partial \boldsymbol{e}_x} \dot{\boldsymbol{e}}_x, \tag{29}$$

$$b_{h_{a,i},min}(t_k) = \min_{\boldsymbol{z} \in S(t_k)} \frac{\partial b(\boldsymbol{y}_1 + \boldsymbol{e}_x, \boldsymbol{y}_2 + \boldsymbol{e}_i)}{\partial \boldsymbol{y}_2} h_{a,i}(\boldsymbol{y}_2), \tag{30}$$

$$b_{E_i,min}(t_k) = \min_{\boldsymbol{z} \in S(t_k)} \frac{\partial b(\boldsymbol{y}_1 + \boldsymbol{e}_x, \boldsymbol{y}_2 + \boldsymbol{e}_i)}{\partial \boldsymbol{e}_i} \dot{\boldsymbol{e}}_i, \tag{31}$$

The above optimizations may be nonlinear programs (NLPs). If the safety constraints are linear, then each optimization is just a LP or QP. However, note that even the NLPs are easy to solve since the constraints are mostly linear, as shown in the case studies of Section 6.

This leaves only one remaining term in (17): if $\frac{\partial b(\boldsymbol{x}, \boldsymbol{y}_i)}{\partial \bar{\boldsymbol{x}}} g_a(\bar{\boldsymbol{x}})$ is independent of $\bar{\boldsymbol{x}}, \boldsymbol{e}_x, \bar{\boldsymbol{y}}_i, \boldsymbol{e}_i$, then we do not need to find its limit value within the bound $\boldsymbol{z} \in S(t_k)$; otherwise, let $\bar{\boldsymbol{x}} = (\bar{x}_1, \dots, \bar{x}_n) \in \mathbb{R}^n$, $\boldsymbol{u} = (u_1, \dots, u_q) \in \mathbb{R}^q$ and $g_a = (g_1, \dots, g_q) \in \mathbb{R}^{n \times q}$. The sign of $u_j(t_k), j \in \{1, \dots, q\}, k = 1, 2 \dots$ can be determined by solving the CBF-based QP (19) at time t_k. We can then determine the limit value $b_{g_j,lim}(t_k) \in \mathbb{R}, j \in \{1, \dots, q\}$ of $\frac{\partial b(\boldsymbol{x}, \boldsymbol{y}_i)}{\partial \bar{\boldsymbol{x}}} g_j(\bar{\boldsymbol{x}})$ by

$$b_{g_j,lim}(t_k) = \begin{cases} \min\limits_{\boldsymbol{z} \in S(t_k)} \dfrac{\partial b(\boldsymbol{y}_1 + \boldsymbol{e}_x, \boldsymbol{y}_2 + \boldsymbol{e}_i)}{\partial \boldsymbol{y}_1} g_j(\boldsymbol{y}_1), & \text{if } u_j(t_k) \ge 0, \\ \max\limits_{\boldsymbol{z} \in S(t_k)} \dfrac{\partial b(\boldsymbol{y}_1 + \boldsymbol{e}_x, \boldsymbol{y}_2 + \boldsymbol{e}_i)}{\partial \boldsymbol{y}_1} g_j(\boldsymbol{y}_1), & \text{otherwise} \end{cases} \tag{32}$$

Let $b_{g_a,lim}(t_k) = (b_{g_1,lim}(t_k), \dots, b_{g_q,lim}(t_k)) \in \mathbb{R}^q$, and we set $b_{g_a,lim}(t_k) = \frac{\partial b(\boldsymbol{x}, \boldsymbol{y}_i)}{\partial \bar{\boldsymbol{x}}} g_a(\bar{\boldsymbol{x}})$ if $\frac{\partial b(\boldsymbol{x}, \boldsymbol{y}_i)}{\partial \bar{\boldsymbol{x}}} g(\bar{\boldsymbol{x}})$ is independent of $\bar{\boldsymbol{x}}, \boldsymbol{e}_x, \bar{\boldsymbol{y}}_i, \boldsymbol{e}_i$ for notational simplicity.

To sum up, the condition that guarantees the satisfaction of (17) in the time interval $(t_k, t_{k+1}]$ is given by

$$\begin{aligned} b_{f_a,min}(t_k) + b_{g_a,lim}(t_k)\boldsymbol{u}(t_k) + b_{e_x,min}(t_k) + b_{h_{a,i},min}(t_k) \\ + b_{e_i,min}(t_k) + b_{\alpha_1,min}(t_k) \ge 0. \end{aligned} \tag{33}$$

We would also like to add the sign condition to the set $S(t_k)$ in order to make this framework work as shown in (32), i.e., we add $\frac{\partial b(\boldsymbol{x}, \boldsymbol{y}_i)}{\partial \bar{\boldsymbol{x}}} g_i(\bar{\boldsymbol{x}}) \ge 0$ if $\frac{\partial b(\boldsymbol{x}, \boldsymbol{y}_i)}{\partial \bar{\boldsymbol{x}}} g_i(\bar{\boldsymbol{x}})$ is positive at time t_k, and vice versa. Note that, despite Assumption 2, it is still possible that $b_{g_a,lim}(t_k) = \boldsymbol{0}$ by (32) as we consider all possible state $\boldsymbol{z} \in S(t_k)$. If (33) is satisfied even without the control component, then the safety is still guaranteed even if we do not consider (33) in the QP. Otherwise, we can deal with it with the approaches discussed after Assumption 2. In this paper, we tune the parameters of the CBF (i.e., how to define a class-$\mathcal{K}$ function of a CBF) and change the reference path (e.g., changing the parameters (such as c_3 in Definition 5) of a CLF) to avoid these possible "singular" states.

In order to apply the above condition (33) to the problem (19), we just replace (17) by (33) and consider the problem at time t_k, i.e., we have a QP:

$$\min_{\boldsymbol{u}(t_k), \delta(t_k)} \|\boldsymbol{u}(t_k)\|^2 + p\delta^2(t_k) \tag{34}$$

subject to (33), (2) and (20). The feasibility of the above QPs can be guaranteed by finding a suitable feasibility constraint, as shown in Xiao, Belta, and Cassandras (2022); briefly, we determine sufficient conditions for feasibility and then enforce them by using another CBF.

Triggering events: Based on the above, we define seven events that determine the condition that triggers an instance of solving the QP (34):

- **Event 1:** $|\boldsymbol{e}_x| \le \boldsymbol{w}$ is about to be violated.
- **Event 2:** $|\dot{\boldsymbol{e}}_x| \le \boldsymbol{\nu}$ is about to be violated.
- **Event 3:** the state of (10) reaches the boundaries of $S_x(t_k)$ in (24).
- **Event 4:** $|\boldsymbol{e}_i| \le \boldsymbol{W}_i$ is about to be violated.
- **Event 5:** $|\dot{\boldsymbol{e}}_i| \le \boldsymbol{V}_i$ is about to be violated.
- **Event 6:** the state of (11) reaches the boundaries of $S_{y,i}(t_k)$ in (25).
- **Event 7:** $\frac{\partial b(\boldsymbol{x}, \boldsymbol{y}_i)}{\partial \bar{\boldsymbol{x}}} g_j(\bar{\boldsymbol{x}}), j \in \{1, \dots, q\}$ changes sign for $t > t_k$ compared to the sign it had at t_k.

In other words, the next time instant $t_{k+1}, k = 1, 2 \dots$ to solve the QP (34) is determined by:

$$\begin{aligned} t_{k+1} = \min\{t > t_k : |\boldsymbol{e}_x(t)| = \boldsymbol{w} \text{ or } |\dot{\boldsymbol{e}}_x(t)| = \boldsymbol{\nu} \\ \text{or } |\bar{\boldsymbol{x}}(t) - \bar{\boldsymbol{x}}(t_k)| = \boldsymbol{s}(\beta_1(b(\boldsymbol{x}(t_k), \boldsymbol{y}_i(t_k)))) \text{ or } |\boldsymbol{e}_i(t)| = \boldsymbol{W}_i \\ \text{or } |\dot{\boldsymbol{e}}_i(t)| = \boldsymbol{V}_i \text{ or } \frac{\partial b(\boldsymbol{x}, \boldsymbol{y}_i)}{\partial \bar{\boldsymbol{x}}} g_j(\bar{\boldsymbol{x}}), j \in \{1, \dots, q\} \text{ changes sign} \\ \text{or } |\bar{\boldsymbol{y}}_i(t) - \bar{\boldsymbol{y}}_i(t_k)| = \boldsymbol{S}_i(\beta_2(b(\boldsymbol{x}(t_k), \boldsymbol{y}_i(t_k)))), i \in S_a\}, \end{aligned} \tag{35}$$

where $t_1 = 0$. Events 1, 2, 4, 5, 7 can be detected by direct sensor measurements, while Events 3, 6 can be detected by monitoring the dynamics (10), (11). The magnitude of each component of $s(\beta_1(b(\boldsymbol{x}(t_k), \boldsymbol{y}_i(t_k))))$, $\boldsymbol{S}_i(\beta_2(b(\boldsymbol{x}(t_k), \boldsymbol{y}_i(t_k))))$ (as well as other bounds) is selected to capture a tradeoff between the time complexity and the conservativeness of this approach: if the magnitude is large, then the number of events is small but this approach is considerably conservative as we determine the condition (33) through the minimum values as in (27)–(32). If $s(\cdot), \boldsymbol{S}_i(\cdot)$ are some constants, then the control system will be too conservative when its state reaches the boundary of the set C_1 as the states of (10) and (11) change slowly at the boundary. However, when the system states are far from the boundary of C_1, i.e., $b(\boldsymbol{x}(t_k), \boldsymbol{y}_i(t_k))$ takes some large value, this again will make the control system too conservative if we take $s(\cdot), \boldsymbol{S}_i(\cdot)$ as a function of $b(\boldsymbol{x}(t_k), \boldsymbol{y}_i(t_k))$. Therefore, we wish to truncate both $s(\cdot), \boldsymbol{S}_i(\cdot)$ in the form:

$$s(\beta_1(b(\boldsymbol{x}(t_k), \boldsymbol{y}_i(t_k)))) = \begin{cases} s_0, \text{ if } s(\beta_1(b(\boldsymbol{x}(t_k), \boldsymbol{y}_i(t_k)))) \geq s_0, \\ s(\beta_1(b(\boldsymbol{x}(t_k), \boldsymbol{y}_i(t_k)))), \text{ otherwise.} \end{cases} \tag{36}$$

$$\boldsymbol{S}_i(\beta_2(b(\boldsymbol{x}(t_k), \boldsymbol{y}_i(t_k)))) = \begin{cases} \boldsymbol{S}_0, \text{ if } \boldsymbol{S}_i(\beta_2(b(\boldsymbol{x}(t_k), \boldsymbol{y}_i(t_k)))) \geq \boldsymbol{S}_0, \\ \boldsymbol{S}_i(\beta_2(b(\boldsymbol{x}(t_k), \boldsymbol{y}_i(t_k)))), \text{ otherwise.} \end{cases} \tag{37}$$

where $s_0 \in \mathbb{R}^n, \boldsymbol{S}_0 \in \mathbb{R}^n$.

Formally, we have the following theorem to show that the satisfaction of the safety constraint (9) is guaranteed for the real unknown dynamics under condition (33):

Theorem 2 (*Xiao, Belta, and Cassandras (2023)*). *Given a HOCBF $b(\boldsymbol{x})$ with $m = 1$ as in Definition 4, let $t_{k+1}, k = 1, 2 \ldots$ be determined by (35) with $t_1 = 0$, and (33) be determined by (27)–(32), respectively. Then, under Assumptions 1–2, any control $\boldsymbol{u}(t_k)$ that satisfies (33) and updates the real unknown dynamics and the adaptive dynamics (10) within time interval $[t_k, t_{k+1})$ renders the set C_1 forward invariant for the real unknown dynamics.*

Remark 2. We could also consider the minimum value of $\frac{\partial b(\boldsymbol{y}_1+\boldsymbol{e}_x, \boldsymbol{y}_2+\boldsymbol{e}_i)}{\partial \boldsymbol{y}_1} f_a(\boldsymbol{y}_1) + \frac{\partial b(\boldsymbol{y}_1+\boldsymbol{e}_x, \boldsymbol{y}_2+\boldsymbol{e}_i)}{\partial \boldsymbol{e}_x} \dot{\boldsymbol{e}}_x + \alpha_1(b(\boldsymbol{y}_1+\boldsymbol{e}_x, \boldsymbol{y}_2+\boldsymbol{e}_i)) + \frac{\partial b(\boldsymbol{y}_1+\boldsymbol{e}_x, \boldsymbol{y}_2+\boldsymbol{e}_i)}{\partial \boldsymbol{y}_2} h_{a,i}(\boldsymbol{y}_2) + \frac{\partial b(\boldsymbol{y}_1+\boldsymbol{e}_x, \boldsymbol{y}_2+\boldsymbol{e}_i)}{\partial \boldsymbol{e}_i} \dot{\boldsymbol{e}}_i$ within the bound $\boldsymbol{z} \in S(t_k)$ instead of considering them separately as in (27)–(32). This will be less conservative (but more computationally expensive) as the constraint (33) is stronger compared with the CBF constraint (17), and we wish to find the largest possible value of the left-hand side of (17) that can support Theorem 2.

Events 1 and 2 will be frequently triggered if the modeling of the adaptive affine dynamics (10) has a large error with respect to the real dynamics of the control system and the same is true for Events 4 and 5. Therefore, we would like to model the adaptive affine dynamics (10) and the adaptive dynamics (11) as accurately as possible in order to reduce the number of events required to solve the QP (34).

State synchronization and adaptation of dynamics An additional important step is to synchronize the state of the real unknown dynamics of the control system with the state of the adaptive affine dynamics in (10) such that we always have $\boldsymbol{e}_x(t_k) = 0$ and make $\dot{\boldsymbol{e}}_x(t_k)$ close to 0. This is done by setting

$$\bar{\boldsymbol{x}}(t_k) = \boldsymbol{x}(t_k), \tag{38}$$

and by updating $f_a(\bar{\boldsymbol{x}}(t))$ in the adaptive affine dynamics (10) right after (t^+) an event occurs at t:

$$f_a(\bar{\boldsymbol{x}}(t^+)) = f_a(\bar{\boldsymbol{x}}(t^-)) + \dot{\boldsymbol{e}}_x(t_i). \tag{39}$$

where t^+, t^- denote instants right after and before t. In this way, the dynamics (10) are adaptively updated at each event, i.e., at $t_k, k = 1, 2, \ldots$. Note that we may also update $g_a(\cdot)$, which is harder than updating $f_a(\cdot)$ since $g_a(\cdot)$ is multiplied by $\boldsymbol{u}$ that is to be determined, i.e., the update of $g_a(\cdot)$ will depend on $\boldsymbol{u}$. We do not consider the update of $g_a(\cdot)$ in this paper, but it does not diminish the validity of the approach. This possibility is the subject of ongoing work.

Along the same lines, we also synchronize the state of agent $i \in S_a$ and (11), by updating $h_{a,i}(\bar{\boldsymbol{y}}_i(t))$ of the adaptive dynamics (11) right after an event occurs at t (i.e., at t^+):

$$\bar{\boldsymbol{y}}_i(t_k) = \boldsymbol{y}_i(t_k), \tag{40}$$

$$h_{a,i}(\bar{\boldsymbol{y}}_i(t^+)) = h_{a,i}(\bar{\boldsymbol{y}}_i(t^-)) + \dot{\boldsymbol{e}}_i(t_j). \tag{41}$$

The control obtained by solving a traditional CBF-based QP is Lipschitz if there are no control bounds (2) (Morris, Powell, & Ames, 2015). However, control bounds exist in our formulation, which is an event-triggered QP. Even so, the safety is still guaranteed in the proposed framework and there exists a minimum inter-event time, as shown next. By (38) and (39), we have that $\boldsymbol{e}_x(t_k) = 0$ and $\dot{\boldsymbol{e}}_x(t_k)$ is close to 0. There exist lower bounds for the occurrence times of Event 1 and Event 3 (the same applies to Events 4 and 6) as the controls are bounded, and they are determined by the limit values of the component of f_a, g_a within X and U, as well as the real unknown dynamics. Assuming the functions that define the real unknown dynamics are Lipschitz continuous, and the functions f_a, g_a in (10) are also assumed to be Lipschitz continuous, it follows that $\dot{\boldsymbol{e}}_x$ is also Lipschitz continuous since $\boldsymbol{u} \in U$. Suppose the largest Lipschitz constant among all the components in $\dot{\boldsymbol{x}}$ is $L, \forall \boldsymbol{x} \in X$, and the smallest Lipschitz constant among all the components in $\dot{\bar{\boldsymbol{x}}}$ is $\bar{L}, \forall \bar{\boldsymbol{x}} \in X$, then the lower bound time for Event 2 is $\frac{\nu_{min}}{L-\bar{L}}$, where $\nu_{min} > 0$ is the minimum component in $\boldsymbol{\nu}$. Similarly, there is also a lower bound time for Events 5 and 7. On the other hand, since the control is constant in each time interval, and there exists a lower bound for the event time, Zeno behavior will not occur. We summarize the event-triggered control scheme in Alg. 1.

Algorithm 1: Event-triggered CBFs

Input: Measurements $\boldsymbol{x}$ and $\dot{\boldsymbol{x}}$ from the controlled agent, measurements $\boldsymbol{y}$ and $\dot{\boldsymbol{y}}_i$ from agent $i \in S_a$, adaptive affine model (10), adaptive model (11), settings for QP (34), $\boldsymbol{w}, \boldsymbol{\nu}, s(\cdot), \boldsymbol{W}_i, \boldsymbol{V}_i, \boldsymbol{S}(\cdot)$.
Output: Event time $t_k, k = 1, 2, \ldots$ and $\boldsymbol{u}^*(t_k)$.

```
k = 1, t_k = 0;
while t_k ≤ T do
    Measure x and ẋ from the controlled agent at t_k;
    Measure y and ẏ_i from agent i ∈ S_a at t_k;
    Sync. the state of (10) and the controlled agent by (38), (39);
    Sync. the state of (11) and agent i by (40),(41);
    Evaluate (27)-(32);
    Solve the QP (34) at t_k and get u*(t_k);
    while t ≤ T do
        Apply u*(t_k) to the controlled agent and (10) for t ≥ t_k;
        Measure x and ẋ from the controlled agent;
        Measure y and ẏ_i from agent i ∈ S_a;
        Evaluate t_{k+1} by (35);
        if t_{k+1} is found with ε > 0 error (i.e., the states reach the
          bounds with ε error in (35)) then
            k ← k + 1, break;
        end
    end
end
```

High-relative-degree constraints In the case of high-relative-degree safety constraints, we have to use HOCBFs instead of CBFs to enforce them. The event-triggered framework for unknown dynamics is similar to the case of relative-degree-one safety constraints. Please refer to Xiao, Belta, and Cassandras (2023) for more details regarding the high-relative-degree case. The measurement uncertainties are more challenging to deal with since higher derivatives of $\boldsymbol{x}$ and $\boldsymbol{y}_i$ are involved in HOCBFs.

5.2. Model-free methods for unknown dynamics

In this subsection, we consider the case where the adaptive dynamics (11) are not necessary for all other agents, but the adaptive affine dynamics (10) are still needed for the ego agent. A model-free method for the ego agent as well is a promising future direction to pursue. The decentralized optimal control for the ego agent is considered in this case, with the event-triggered CBF framework becoming simpler than that in the last section, as shown in the sequel.

Since $\boldsymbol{e}_i = \boldsymbol{y}_i - \bar{\boldsymbol{y}}_i$, (15) can be rewritten in the form:

$$\begin{aligned}\frac{db(\bar{\boldsymbol{x}}+\boldsymbol{e}_x, \boldsymbol{y}_i)}{dt} = \frac{\partial b(\bar{\boldsymbol{x}}+\boldsymbol{e}_x, \boldsymbol{y}_i)}{\partial \bar{\boldsymbol{x}}}\dot{\bar{\boldsymbol{x}}} + \frac{\partial b(\bar{\boldsymbol{x}}+\boldsymbol{e}_x, \boldsymbol{y}_i)}{\partial \boldsymbol{e}_x}\dot{\boldsymbol{e}}_x \\ + \frac{\partial b(\bar{\boldsymbol{x}}+\boldsymbol{e}_x, \boldsymbol{y}_i)}{\partial \boldsymbol{y}_i}\dot{\boldsymbol{y}}_i,\end{aligned} \tag{42}$$

where $\boldsymbol{y}_i$ and $\dot{\boldsymbol{y}}_i$ are directly obtained from sensor measurements. Similar to (17), combining (42), (10) and (16), we get the CBF constraint that guarantees (9):

$$\begin{aligned}\frac{\partial b(\boldsymbol{x}, \boldsymbol{y}_i)}{\partial \bar{\boldsymbol{x}}} f_a(\bar{\boldsymbol{x}}) + \frac{\partial b(\boldsymbol{x}, \boldsymbol{y}_i)}{\partial \bar{\boldsymbol{x}}} g_a(\bar{\boldsymbol{x}})\boldsymbol{u} + \frac{\partial b(\boldsymbol{x}, \boldsymbol{y}_i)}{\partial \boldsymbol{e}_x}\dot{\boldsymbol{e}}_x \\ + \frac{\partial b(\boldsymbol{x}, \boldsymbol{y}_i)}{\partial \boldsymbol{y}_i}\dot{\boldsymbol{y}}_i + \alpha_1(b(\boldsymbol{x}, \boldsymbol{y}_i)) \geq 0.\end{aligned} \tag{43}$$

In the event-triggered control framework, we formulate the CBF-based problem as in (19) by replacing (17) with (43). In addition to defining the bounds for $e_{x,j}$ and $\dot{e}_{x,j}$ as in (21) and the bound for the state bound for $\bar{\boldsymbol{x}}$ as in the set (24), we only need to define bounds for $\boldsymbol{y}_i, \dot{\boldsymbol{y}}_i$ in the form:

$$|\boldsymbol{y}_i| \leq \boldsymbol{W}_i, \qquad |\dot{\boldsymbol{y}}_i| \leq \boldsymbol{V}_i, \qquad i \in S_a. \tag{44}$$

where the inequalities are interpreted componentwise, and $\boldsymbol{W}_i \in \mathbb{R}^n_{>0}, \boldsymbol{V}_i \in \mathbb{R}^n_{>0}$. Note that the above bounds can also be defined in the adaptive form as in (23) by making the bound values dependent on the value of the CBF.

Let $\boldsymbol{z} := (\boldsymbol{y}_1, \boldsymbol{e}_x, \dot{\boldsymbol{e}}_x, \boldsymbol{y}_i, \dot{\boldsymbol{y}}_i)$, where $\boldsymbol{y}_1 \in S_x(t_k)$. We then define an overall set $S(t_k)$:

$$\begin{aligned}S(t_k) = \{\boldsymbol{z} \in \mathbb{R}^{5n} : \boldsymbol{y}_1 \in S_x(t_k), |\boldsymbol{e}_x| \leq \boldsymbol{w}, \\ |\dot{\boldsymbol{e}}_x| \leq \boldsymbol{v}, |\boldsymbol{y}_i| \leq \boldsymbol{W}_i, |\dot{\boldsymbol{y}}_i| \leq \boldsymbol{V}_i, \\ (\boldsymbol{y}_1 + \boldsymbol{e}_x, \boldsymbol{y}_i) \in C_1, i \in S_a\}.\end{aligned} \tag{45}$$

Compared to $\boldsymbol{z}$ in (26), the dimension of $\boldsymbol{z}$ is now decreased by n.

Next, we can find the minimum values $b_{f_a,min}(t_k)$, $b_{\alpha_1,min}(t_k)$, $b_{e,min}(t_k)$ of $\frac{\partial b(\bar{\boldsymbol{x}}+\boldsymbol{e}_x, \boldsymbol{y}_i)}{\partial \bar{\boldsymbol{x}}} f_a(\bar{\boldsymbol{x}})$, $\alpha_1(b(\boldsymbol{x}, \boldsymbol{y}_i))$, $\frac{\partial b(\boldsymbol{x}, \boldsymbol{y}_i)}{\partial \boldsymbol{e}_x}\dot{\boldsymbol{e}}_x$, respectively, for the preceding time interval $[t_k, t_{k+1}]$ that satisfy $\boldsymbol{z} \in S(t_k)$ starting at time t_k as in (27)–(29). The minimum value $b_{y_i,min}(t_k) \in \mathbb{R}$ of $\frac{\partial b(\boldsymbol{x}, \boldsymbol{y}_i)}{\partial \boldsymbol{y}_i}\dot{\boldsymbol{y}}_i, i \in S_a$ is given by

$$b_{y_i,min}(t_k) = \min_{\boldsymbol{z} \in S(t_k)} \frac{\partial b(\boldsymbol{y}_1 + \boldsymbol{e}_x, \boldsymbol{y}_i)}{\partial \boldsymbol{y}_i}\dot{\boldsymbol{y}}_i, \tag{46}$$

The limit value of the coefficient of the control in the CBF constraint is also found as in (32).

Finally, the condition that guarantees the satisfaction of (43) in the time interval $(t_k, t_{k+1}]$ is given by

$$\begin{aligned}b_{f_a,min}(t_k) + b_{g_a,lim}(t_k)\boldsymbol{u}(t_k) + b_{e_x,min}(t_k) \\ + b_{y_i,min}(t_k) + b_{\alpha_1,min}(t_k) \geq 0.\end{aligned} \tag{47}$$

The above condition is added to the CBF-based problem (34) by replacing (33) with (47).

Triggering events: Based on the above, we define six events that determine the condition that triggers an instance of solving the QP (34) (replacing (33) with (47)):

- **Event 1:** $|\boldsymbol{e}_x| \leq \boldsymbol{w}$ is about to be violated.
- **Event 2:** $|\dot{\boldsymbol{e}}_x| \leq \boldsymbol{v}$ is about to be violated.
- **Event 3:** the state of (10) reaches the boundaries of $S_x(t_k)$ in (24).
- **Event 4:** $|\boldsymbol{y}_i| \leq \boldsymbol{W}_i$ is about to be violated.
- **Event 5:** $|\dot{\boldsymbol{y}}_i| \leq \boldsymbol{V}_i$ is about to be violated.
- **Event 6:** $\frac{\partial b(\boldsymbol{x}, \boldsymbol{y}_i)}{\partial \bar{\boldsymbol{x}}} g_j(\bar{\boldsymbol{x}}), j \in \{1, \dots, q\}$ changes sign for $t > t_k$ compared to the sign it had at t_k.

Note that Event 6 is not necessary since it would not affect the validity of the condition (47). We add this event here since we observe that the system behavior usually changes (e.g., from acceleration to brake in a vehicle) when the sign of the control coefficient in a CBF changes.

In other words, the next time instant $t_{k+1}, k = 1, 2 \dots$ to solve the QP is determined by:

$$\begin{aligned}t_{k+1} = \min\{t > t_k : |\boldsymbol{e}_x(t)| = \boldsymbol{w} \text{ or } |\dot{\boldsymbol{e}}_x(t)| = \boldsymbol{v} \text{ or } |\boldsymbol{y}_i(t)| = \boldsymbol{W}_i \\ \text{or } |\bar{\boldsymbol{x}}(t) - \bar{\boldsymbol{x}}(t_k)| = s(\beta_1(b(\boldsymbol{x}(t_k), \boldsymbol{y}_i(t_k)))) \text{ or } |\dot{\boldsymbol{y}}_i(t)| = \boldsymbol{V}_i \\ \text{or } \frac{\partial b(\boldsymbol{x}, \boldsymbol{y}_i)}{\partial \bar{\boldsymbol{x}}} g_j(\bar{\boldsymbol{x}}), j \in \{1, \dots, q\} \text{ changes sign}, i \in S_a\},\end{aligned} \tag{48}$$

where $t_1 = 0$.

We can then prove the safety guarantees under the proposed robust framework as in Theorem 2. We only need to synchronize the state and update the dynamics for the ego agent as in (38) and (39). An algorithm similar to Alg. 1 can also be obtained to summarize process.

5.3. Human in the loop

Our robust control framework is a natural fit for incorporating human agents in the loop of multi-agent systems, since we do not need to know the dynamics of those agents or the control policy they adopt. Human agents may control any one or more agents $i \in S_a$. We may just treat those human agents as "blackbox" models and policies, and use sensors to measure system states (and their derivatives) required in the event-triggered CBFs that enforce safety. We note that the common interpretation of "human in the loop" control is to view a human as participating in an otherwise automated control system. Our consideration is a bit different because our focus is on *multi-agent systems*, in which case a natural point of view is to consider some agents as uncontrollable "humans" and others as cooperating automated controllable ones. The human agents participate in the system-wide control loop in which the goal is to achieve optimal and safe system-wide (social) operation. The autonomous agents need to interact with human-controlled agents in a safety-guaranteed way using the proposed event-triggered CBF-based method.

A major challenge in the proposed framework involves the sensor measurements it requires since it is usually difficult to measure the derivatives of system states, especially for high relative degree safety constraints $b(\boldsymbol{x}, \boldsymbol{y}_i) \geq 0$ that are enforced by HOCBFs in the following form:

$$\begin{aligned}\frac{\partial^m b(\boldsymbol{x}, \boldsymbol{y}_i)}{\partial \bar{\boldsymbol{x}}^m} f_a^{[m]}(\bar{\boldsymbol{x}}) + \frac{\partial^m b(\boldsymbol{x}, \boldsymbol{y}_i)}{\partial \bar{\boldsymbol{x}}^m} f_a^{[m-1]}(\bar{\boldsymbol{x}}) g_a^{[1]}(\bar{\boldsymbol{x}})\boldsymbol{u} \\ + \frac{\partial^m b(\boldsymbol{x}, \boldsymbol{y}_i)}{\partial \boldsymbol{e}_x^m}\boldsymbol{e}_x^{(m)} + \frac{\partial^m b(\boldsymbol{x}, \boldsymbol{y}_i)}{\partial \boldsymbol{e}_i^m}\boldsymbol{y}_i^{(m)} \\ + R(b(\boldsymbol{x}, \boldsymbol{y}_i)) + \alpha_m(\psi_{m-1}(\boldsymbol{x}, \boldsymbol{y}_i)) \geq 0,\end{aligned} \tag{49}$$

where $\frac{\partial^m b(\boldsymbol{x}, \boldsymbol{y}_i)}{\partial \bar{\boldsymbol{x}}^m} f_a^{[m]}(\bar{\boldsymbol{x}})$ denotes the m times partial derivative of the function $b(\boldsymbol{x}, \boldsymbol{y}_i)$ w.r.t. $\bar{\boldsymbol{x}}$ along $f_a(\bar{\boldsymbol{x}})$ (a similar definition to the Lie derivative in Definition 4), and we have similar definitions for $\frac{\partial^m b(\boldsymbol{x}, \boldsymbol{y}_i)}{\partial \bar{\boldsymbol{x}}^m} f_a^{[m-1]} g_a^{[1]}(\bar{\boldsymbol{x}})\boldsymbol{u}$. The above constraint would also involve human control if agent i is a human controlled agent and if we model such an agent using adaptive affine dynamics similar to (10). In this way, we can consider safe human-autonomous system interactions. In this work, we do not explicitly study or infer human control policies, thus, we treat human-controlled agents as having unknown dynamics. Further studies regarding safe human-autonomous system interactions (such as in a game-theoretic manner) are needed in future work.

In (49), $R(b(\boldsymbol{x}, \boldsymbol{y}_i))$ also contains the remaining time derivatives of $\boldsymbol{e}_x$ and $\boldsymbol{y}_i$ with degree less than m, while $\boldsymbol{e}_x^{(j)} = \boldsymbol{x}^{(j)} - \bar{\boldsymbol{x}}^{(j)}, \boldsymbol{y}_i^{(j)}, j \in \{1, \dots, m\}$ is the jth derivative and is evaluated online by $\boldsymbol{x}^{(j)}$ (from a sensor) of the real system and by $\boldsymbol{y}_i^{(j)}$ (from a sensor) of system $i \in S_a$ and

$\bar{\boldsymbol{y}}_i^{(j)}$ of (11), respectively. Those derivatives are in general intractable to estimate. In order to address this, we propose methods for relative degree reduction in the CBF method as a potential research direction, as discussed in the next subsection.

5.4. CBF relative degree reduction

As mentioned in the last subsection, when dealing with high relative degree safety constraints, we have to differentiate the safety constraints more than once in order to get the control in the corresponding derivative. As a result, high order derivatives of $\boldsymbol{y}_i$ are also involved. This makes the sensor measurements intractable in most cases, as the measurement of high order derivatives of system states is extremely difficult in practice. However, we can avoid this problem through systematic ways to achieve relative degree reduction in CBFs. In other words, we can *transform* the relative degree of a safety constraint to one by adding an extra term to the safety constraint at the cost of potential conservativeness.

For instance, we can transform the safety constraint $x - x_p \geq l_0$ to $x - x_p \geq \varphi v + l_0$ in an adaptive cruise control problem, where double integrator dynamics are considered, and x, x_p denotes the along lane position of the ego vehicle and its preceding vehicle, v denotes the speed of the ego vehicle, and $\varphi > 0, l_0 > 0$ are constants. In this case, the transformed safety constraint has relative degree one (while the original safety constraint has relative degree two), and the satisfaction of the transformed constraint implies the satisfaction of the original constraint (as $v > 0$ in general). Through relative degree reduction, we only need to measure $\boldsymbol{y}_i$ and $\dot{\boldsymbol{y}}_i$, which is much more tractable than the high-order case.

Formally, we consider the case where the full dynamics (1) are known (this assumption can be relaxed by the proposed event-triggered CBFs). In the HOCBF method, we directly define $b(\boldsymbol{x}, \boldsymbol{y}_i)$ in (9) as a HOCBF in order to enforce this safety constraint. Here, instead, we define a transformation function $T_V : \mathbb{R}^n \to \mathbb{R}$ in the form:

$$T_V(\boldsymbol{x}, \boldsymbol{y}_i) = b(\boldsymbol{x}, \boldsymbol{y}_i) - V(\boldsymbol{x}), \tag{50}$$

where $V : \mathbb{R}^{2n} \to \mathbb{R}$ is a positive definite function in the form:

$$V(\boldsymbol{x}) = \boldsymbol{x}^T P \boldsymbol{x}, \tag{51}$$

where $P \in \mathbb{R}^{n \times n}$ is positive definite. $V(\boldsymbol{x})$ has relative degree one since all the state variables in $\boldsymbol{x}$ show up. We may define $V(\boldsymbol{x})$ to be any other continuously differentiable function that has relative degree one, and use a CBF to ensure it is non-negative. For simplicity, we usually consider it to be quadratic.

Then, we can define $T_V(\boldsymbol{x}, \boldsymbol{y}_i)$ as a CBF since its relative degree is also only one due to the transformation (50). We may define $V(\boldsymbol{x})$ to be singular-free, i.e. $L_g V(\boldsymbol{x}) \neq 0$ for all $\boldsymbol{x}$ such that $b(\boldsymbol{x}, \boldsymbol{y}_i) = 0$, in the form $V(\boldsymbol{x}) = (\boldsymbol{x} + c)^T P(\boldsymbol{x} + c)$, where $c \in \mathbb{R}$ is properly chosen to satisfy this condition. This shows the advantage of using a transformation method in enforcing safety, as it gives us the freedom to design the function $V(\boldsymbol{x})$ such that the singularity problem can be avoided, something that is hard to address in the original CBF/HOCBF method.

The CBF constraint corresponding to the transformation $T_V(\boldsymbol{x}, \boldsymbol{y}_i)$ is then given by:

$$\begin{aligned} L_f T_V(\boldsymbol{x}, \boldsymbol{y}_i) + L_g T_V(\boldsymbol{x}, \boldsymbol{y}_i)\boldsymbol{u} + \frac{\partial T_V(\boldsymbol{x}, \boldsymbol{y}_i)}{\partial \boldsymbol{y}_i}\dot{\boldsymbol{y}}_i \\ + \alpha(T_V(\boldsymbol{x}, \boldsymbol{y}_i)) \geq 0, \end{aligned} \tag{52}$$

where $\alpha(\cdot)$ is a class $\mathcal{K}$ function. The above equation can ensure $T_V(\boldsymbol{x}, \boldsymbol{y}_i) \geq 0$ by Theorem 1. Since $V(\boldsymbol{x}) \geq 0$, it follows that $b(\boldsymbol{x}, \boldsymbol{y}_i) \geq 0$ is guaranteed.

Conservativeness. One obvious problem with the transformation approach above is that the system could be too conservative, as $b(\boldsymbol{x}, \boldsymbol{y}_i) \geq V(\boldsymbol{x})$ is always true, especially when the value of $V(\boldsymbol{x})$ is large. One approach to address this problem is to define $V(\boldsymbol{x})$ as a CLF such that it decreases to a small value when the system near the safe set boundary. Another way to address this problem is by introducing a penalty on the function $V(\boldsymbol{x})$, similar to the concept of adaptive CBFs (Xiao, Belta, & Cassandras, 2021a). All these ideas and resulting methodologies are open and challenging questions that are worth investigating.

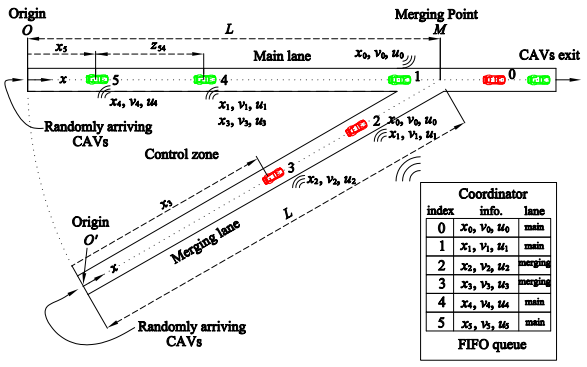

Fig. 3. The merging problem, a collision may happen at the merging point.

6. Applications

In this section, we consider two classes of problems where the proposed approach is applied: a decentralized traffic merging control problem, and a lane merging control problem in highway driving with humans in the loop. All computations and simulations were conducted in MATLAB. We used quadprog to solve the quadratic programs and ode45 to integrate the dynamics.

6.1. Decentralized traffic merging in a bottleneck area

The merging problem arises when traffic must be joined from two roads, usually associated with a main lane and a merging lane as shown in Fig. 3. We consider the case where all traffic consists of vehicles randomly arriving at the two lanes joined at the Merging Point (MP) M. The segment from the origin O or O' to the merging point M has a length L for both lanes, and is called the control zone. In order to share or obtain other vehicle information, each vehicle can use its onboard sensors or communicate with a coordinator associated with the MP whose main function is to collect and share vehicle states. A more detailed merging problem setup is given in Xiao and Cassandras (2021). In contrast to the problem considered in Xiao and Cassandras (2021) where the vehicle dynamics are assumed known, in real traffic merging each vehicle does not know the dynamics of other vehicles and may also not have accurate dynamics of its own. Therefore, the safe merging constraint becomes critical and hard to be guaranteed.

The real dynamics for i are *unknown* to the controller:

$$\dot{x}_i(t) = \sigma_{i,1}(t) + v_i(t), \;\; \dot{v}_i(t) = \sigma_{i,2}(t) + \sigma_{i,3}(t)u_i(t), \tag{53}$$

where $\boldsymbol{x}_i = (x_i, v_i)$ and $x_i(t)$ denotes the along lane distance of vehicle i with respect to the origin, $v_i(t)$ denotes its the velocity, and $u(t)$ is its control (acceleration). $\sigma_1(t), \sigma_2(t), \sigma_3(t)$ denote three random processes whose pdf's have finite support.

As in Xiao and Cassandras (2021), we consider the following double integrator as the initial adaptive model:

$$\dot{\bar{x}}_i(t) = h_{i,1}(t) + \bar{v}_i(t), \quad \dot{\bar{v}}_i(t) = h_{i,2}(t) + u_i(t), \tag{54}$$

where $\bar{\boldsymbol{x}}_i = (\bar{x}_i, \bar{v}_i)$. $h_{i,1}(t) \in \mathbb{R}, h_{i,2}(t) \in \mathbb{R}$ denote the two adaptive terms in (39), $h_{i,1}(0) = 0, h_{i,2}(0) = 0$.

The objective is to jointly minimize the travel time and energy consumption for each vehicle i in the form $\int_{t_i^0}^{t_i^m} \left(\beta + u_i^2(t)\right) dt$, where t_i^0, t_i^m denote the arrival time of vehicle i at the origin and at the merging

point M, respectively. $\beta > 0$ is a weight parameter that captures the time-energy consumption trade-off. The rear-end safety constraint between vehicle i and its preceding vehicle i_p is similar to the ACC example. For simplicity, we only consider the safe merging constraints for two CAVs $i, i-1$ coming from different roads:

$$x_{i-1}(t_i^m) - x_i(t_i^m) \geq \varphi v_i(t_i^m) + l_0 \tag{55}$$

where $\varphi > 0$ is the headway time and $l_0 \geq 0$. For simplicity, we consider high speed traffic merging, and take $l_0 = 0$. In order to use the CBF method to implement the above safe merging constraint, we convert it to a continuously differentiable constraint:

$$x_{i-1}(t) - x_i(t) \geq \varphi \frac{x_i(t)}{L} v_i(t), \forall t \in [t_i^0, t_i^m], \tag{56}$$

where $x_{i-1}(t) - x_i(t) \geq 0$ when $x_i(t) = 0$, which means the two vehicles $i-1, i$ are allowed arrive at the same time at the origins O and O', respectively. Moreover, note that $x_{i-1}(t) - x_i(t) \geq \varphi v_i(t)$ when $x_i(t) = L$, which satisfies the safe merging constraint (55) when i arrives at the merging point M ($i-1$ has already passed the merging point).

We take i as the ego vehicle in the merging problem. We assume vehicle $i-1$ is under unconstrained optimal control (Xiao & Cassandras, 2021), and vehicle i takes the unconstrained optimal control as a reference. Vehicle i does not know its own dynamics, as well as those of $i-1$. In order to implement the continuous version of the safe merging constraint (56), we define a CBF $b(\boldsymbol{x}_i, \boldsymbol{x}_{i-1}) = x_{i-1}(t) - x_i(t) - \varphi \frac{x_i(t)}{L} v_i(t)$. The relative degree of this CBF is only one with respect to (53). We choose $\alpha_1(b(\boldsymbol{x}_i, \boldsymbol{x}_{i-1})) = b(\boldsymbol{x}_i, \boldsymbol{x}_{i-1})$ in Definition 4. The CBF constraint (5) which in this case is (with respect to the real dynamics (53)): $\dot{b}(\boldsymbol{x}_i, \boldsymbol{x}_{i-1}) + b(\boldsymbol{x}_i, \boldsymbol{x}_{i-1}) \geq 0$. Combining (13), (54) and this constraint, we have

$$\begin{aligned} &\bar{v}_{i-1} + h_{i-1,1} + \dot{e}_{x_{i-1}} - \bar{v}_i - h_{i,1} - \dot{e}_{x_i} \\ &-\frac{\varphi}{L}(\bar{v}_i + h_{i,1} + \dot{e}_{x_i})(\bar{v}_i + e_{v_i}) - \frac{\varphi}{L}(\bar{x}_i + e_{x_i})(u_i + h_{i,2} + \dot{e}_{v_i}) \\ &+\bar{x}_{i-1} + e_{x_{i-1}} - \bar{x}_i - e_{x_i} - \frac{\varphi}{L}(\bar{x}_i + e_{x_i})(\bar{v}_i + e_{v_i}) \geq 0, \end{aligned} \tag{57}$$

where $e_{x_{i-1}} = x_{i-1} - \bar{x}_{i-1}, e_{x_i} = x_i - \bar{x}_i, e_{v_i} = v_i - \bar{v}_i$.

The vehicles may arrive at the origins at the same time, i.e., $b(\boldsymbol{x}_i, \boldsymbol{x}_{i-1})$ may be initially close to 0. Thus, we take $\boldsymbol{s}(\cdot), \boldsymbol{S}_i(\cdot)$ in (23) to be some constant vectors. Similar to (23), we consider the state and bound the errors at step $t_k, k = 1, 2\ldots$ for the above CBF constraint in the form:

$$\begin{aligned} &\bar{x}_{i-1}(t_k) - S_1 \leq \bar{x}_{i-1} \leq \bar{x}_{i-1}(t_k) + S_1, \\ &\bar{v}_{i-1}(t_k) - S_2 \leq \bar{v}_{i-1} \leq \bar{v}_{i-1}(t_k) + S_2, \\ &\bar{x}_i(t_k) - s_1 \leq \bar{x}_i \leq \bar{x}_i(t_k) + s_1, \bar{v}_i(t_k) - s_2 \leq \bar{v}_i \leq \bar{v}_i(t_k) + s_2, \\ &|e_{x_{i-1}}| \leq W, \quad |\dot{e}_{x_{i-1}}| \leq V, \\ &|e_{x_i}| \leq w_1, \quad |\dot{e}_{x_i}| \leq v_1, \quad |e_{v_i}| \leq w_2, \quad |\dot{e}_{v_i}| \leq v_2 \end{aligned} \tag{58}$$

where $S_1 > 0, S_2 > 0, s_1 > 0, s_2 > 0, W > 0, w_1 > 0, w_2 > 0, V > 0, v_1 > 0, v_2 > 0$.

Motivated by (38)–(41), we synchronize the state and update the adaptive dynamics (54) at step $t_k, k = 1, 2\ldots$ in the form:

$$\begin{aligned} &\bar{x}_{i-1}(t_k) = x_{i-1}(t_k), \ \bar{v}_{i-1}(t_k) = v_{i-1}(t_k), \ \bar{x}_i(t_k) = x_i(t_k), \\ &\bar{v}_i(t_k) = v_i(t_k), \quad h_{i-1,1}(t^+) = h_{i-1,1}(t^-) + \sum_{i=0}^{k} \dot{e}_{x_{i-1}}(t_i), \\ &h_{i,1}(t^+) = h_{i,1}(t^-) + \sum_{i=0}^{k} \dot{e}_{x_i}(t_i), h_{i,2}(t^+) = h_{i,2}(t^-) + \sum_{i=0}^{k} \dot{e}_{v_i}(t_i), \end{aligned} \tag{59}$$

where $\dot{e}_{x_{i-1}}(t_k) = \dot{x}_{i-1}(t_k) - (\bar{v}_{i-1}(t_k) + h_{i-1,1}(t_k))$, $\dot{e}_{x_i}(t_k) = \dot{x}_i(t_k) - (\bar{v}_i(t_k) + h_{i,1}(t_k))$, $\dot{e}_{v_i}(t_k) = \dot{v}_i(t_k) - (u_i(t_k^-) + h_{i,2}(t_k))$, $u(t_k^-) = u(t_{k-1})$ and $u(t_0) = 0$. $\dot{x}_{i-1}(t_k), \dot{x}_i(t_k), \dot{v}_i(t_k)$ are estimated by a sensor that measures the real dynamics (53) of $i-1, i$ at time t_k.

Then, we can find the limit values as in (27)–(32), solve the QP (34) at each time step $t_k, k = 1, 2\ldots$, and evaluate the next time step t_{k+1} by (35) afterwards. In the evaluation of t_{k+1}, we have $e_{x_{i-1}} = x_{i-1} - \bar{x}_{i-1}, e_{x_i} = x_i - \bar{x}_i, e_{v_i} = v_i - \bar{v}_i$, $\dot{e}_{x_{i-1}} = \dot{x}_{i-1} - (\bar{v}_{i-1} + h_{i-1,1})$, $\dot{e}_{x_i} = \dot{x}_i - (\bar{v}_i + h_{i,1})$, $\dot{e}_{v_i} = \dot{v}_i - (u_i + h_{i,2})$, where $x_{i-1}, x_i, v_i, \dot{x}_{i-1}, \dot{x}_i, \dot{v}_i$ are estimated by a sensor that measures the real dynamics of $i-1, i$, and $u(t_k)$ is already obtained by solving the QP (34) and is held as a constant until we find t_{k+1}. The optimizations (27)–(32) are NLPs due to the nonlinearity of the CBF $b(\boldsymbol{x}_i, \boldsymbol{x}_{i-1})$. Each NLP can be solved with a computational time of about $0.03s$ using fmincon in MATLAB, and each QP can be solved within $0.01s$ using quadprog in MATLAB (Intel(R) Core(TM) i7-8700 CPU @3.2GHz×2).

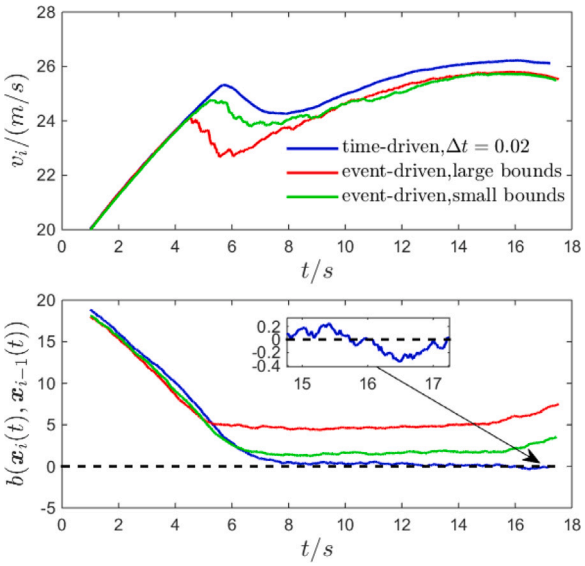

Fig. 4. Comparison between the proposed event-driven method and the time-driven method in guaranteeing the satisfaction of the safe merging constraint for vehicles $i, i-1$. $b(\boldsymbol{x}_i, \boldsymbol{x}_{i-1}) \geq 0$ denotes the forward invariance of C_1, i.e., the satisfaction of the safe merging constraint (under the event driven method). In the small-bounds case, all the state and error bound values are 20% of the ones in the large-bounds case (default values).

In the simulation, the initial speeds of vehicles $i-1, i$ are 18 m/s, 20 m/s with arrival times $0s, 1s$ at the origin O or O', respectively. Other simulation parameters are $\beta = 2.666, \varphi = 1.8s, L = 400$ m, $S_1 = 0.5$ m, $S_2 = 0.2$ m/s, $s_1 = 0.5$ m, $s_2 = 0.2$ m/s, $W = 0.6$ m, $V = 0.3$ m/s, $w_1 = 0.6$ m, $w_2 = 0.3$ m/s, $v_1 = 0.3$ m/s, $v_2 = 0.2$ m/s^2.

The pdf's of $\sigma_1(t), \sigma_2(t), \sigma_3(t)$ are uniform over the intervals $[-2, 2]$ m/s, $[-0.2, 0.2]$ m/s^2, $[0.9, 1.1]$, respectively. The sensor sampling rate is 100 Hz. We compare the proposed event-driven framework with the time-driven approach ($\Delta t = 0.02s$) that takes double integrator as vehicle dynamics.

The simulation results are shown in Fig. 4. Note that, in order to improve the computation efficiency while staying close to optimal solutions, we employed the joint optimal control and barrier function method. As expected, the safe merging constraint between i and $i-1$ is not satisfied with the time-driven method (blue curves shown in Fig. 4) due to the unknown dynamics of both i and $i-1$. The safe merging constraint for i and $i-1$ is guaranteed when using the event-driven approach, as the red curves shown in Fig. 4, but vehicle i tends to be conservative when it approaches the merging point. In order to alleviate this conservativeness, we consider a small-bound case in which the state and error bound values are 20% of the default values, as the green curves shown in Fig. 4.

6.2. Lane changing control with human in the loop

The highway lane-changing scenario (more details are given in Li, Cassandras, and Xiao (2023)) is shown in Fig. 5, where the green vehicles 1 and C are assumed to be cooperating Connected Automated Vehicles (CAVs), the red vehicle H is an uncontrollable Human Driven Vehicle (HDV), and the gray vehicle U is considered as a dynamic

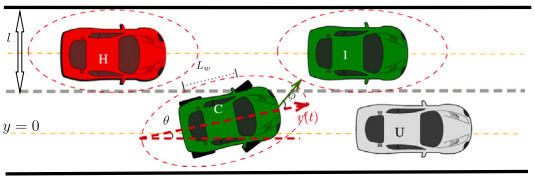

Fig. 5. The basic lane-changing maneuver process. The red vehicle is an HDV, green vehicles are CAVs, and the gray vehicle is a slow-moving and uncontrollable vehicle. (For interpretation of the references to color in this figure legend, the reader is referred to the web version of this article.)

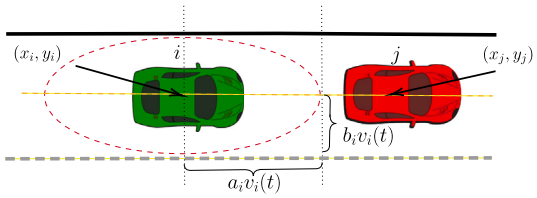

Fig. 6. Definition of an elliptical safe region.

obstacle moving at a slower speed than CAVs. A lane-changing maneuver is triggered by C when an obstacle ahead is detected. In general, such a maneuver can be initiated at any arbitrary time set by C. The framework proposed in this paper can be used in any conflict area involving vehicle interactions, but we limit ourselves to this lane-changing setting which we view as the most challenging among them. We aim to minimize the maneuver time and energy expended, while alleviating any disruption to the fast lane traffic flow. Moreover, considering the presence of HDVs, C also needs to be aware of the behavior of its surrounding HDVs in order to guarantee safety.

Vehicle Dynamics. The dynamics and control policy of the HDV are unknown in this case. Assume the slow vehicle U keeps traveling in the slow lane with a constant speed v_U. For each CAV in Fig. 5, indexed by $i \in \{1, C\}$, its dynamics take the form

$$\underbrace{\begin{bmatrix} \dot{x}_i \\ \dot{y}_i \\ \dot{\theta}_i \\ \dot{v}_i \end{bmatrix}}_{\dot{\boldsymbol{x}}_i} = \underbrace{\begin{bmatrix} v_i \cos\theta_i \\ v_i \sin\theta_i \\ 0 \\ 0 \end{bmatrix}}_{f(\boldsymbol{x}_i(t))} + \underbrace{\begin{bmatrix} 0 & -v_i \sin\theta_i \\ 0 & v_i \cos\theta_i \\ 0 & v_i / L_w \\ 1 & 0 \end{bmatrix}}_{g(\boldsymbol{x}_i(t))} \underbrace{\begin{bmatrix} u_i \\ \phi_i \end{bmatrix}}_{\boldsymbol{u}_i(t)} \tag{60}$$

where $x_i(t), y_i(t), \theta_i(t), v_i(t)$ represent the current longitudinal position, lateral position, heading angle, and speed, respectively. $u_i(t)$ and $\phi_i(t)$ are the acceleration and steering angle (controls) of vehicle i at time t, respectively, $g(\boldsymbol{x}_i(t)) = [g_u(\boldsymbol{x}_i(t)), g_\phi(\boldsymbol{x}_i(t))]$. The maneuver starts at time t_0 and ends at time t_f when C has completely switched to the target lane. The control input and speed for all vehicles are constrained as follows:

$$\boldsymbol{u}_{i_{\min}} \le \boldsymbol{u}_i(t) \le \boldsymbol{u}_{i_{\max}}, \; v_{i_{\min}} \le v_i(t) \le v_{i_{\max}}, \; i \in \{1, C\}, \tag{61}$$

where $\boldsymbol{u}_{i_{\min}}, \boldsymbol{u}_{i_{\max}} \in \mathbb{R}^2$ denote the minimum and maximum control bounds for vehicle i, respectively. $v_{i_{\min}} > 0$ and $v_{i_{\max}} > 0$ are vehicle i's allowable minimum and maximum speed. Setting l as the width of the road, $y = 0$ axis is the center of the slow lane in Fig. 5, we have $y_C(t_0) = 0$, and the lateral positions of vehicles satisfy

$$-\frac{l}{2} \le y_i(t) \le \frac{3}{2} l, \; i \in \{1, C\}. \tag{62}$$

Safety Constraints. Similar to the longitudinal safe distance described in Xiao, Cassandras, and Belta (2023), we define an ellipsoidal safe region $b_{i,j}(\boldsymbol{x}_i, \boldsymbol{x}_j)$ for vehicles i and j during the entire maneuver:

$$b_{i,j} := \frac{(x_j(t) - x_i(t))^2}{(a_i v_i(t))^2} + \frac{(y_j(t) - y_i(t))^2}{(b_i v_i(t))^2} - 1 \ge 0, \tag{63}$$

where j is i's neighboring vehicle, a_i, b_i are weights adjusting the length of the major and minor axes of the ellipse shown in Fig. 6, and the size of the safe region depends on speed, which is one of the relative degree reduction methods. Otherwise, the relative degree of the safety constraint is two, and we need to measure the second derivative of the positions. Note that $b_{i,j}$ is specified from the center of vehicle i to the center of j. In other words, the center of vehicle j must remain outside of i's safe region during the entire maneuver. Defining an elliptical safe region considers the 2D safe distance between two vehicles. Since (63) depends on speed, its CBF constraint only has relative degree one (i.e., we only need to take the derivative of the safety constraint along the dynamics once until the control explicitly shows in the derivative), implying lower complexity in CBF design.

Therefore, CAV $i \in \{1, C\}$ in Fig. 5 must satisfy the following constraints to guarantee safety during any lane change maneuver:

$$b_{C,H} = \frac{(x_C(t) - x_H(t))^2}{a_C^2} + \frac{(y_C(t) - y_H(t))^2}{b_C^2} - v_C^2(t) \ge 0, \tag{64a}$$

$$b_{1,C} = \frac{(x_1(t) - x_C(t))^2}{a_1^2} + \frac{(y_1(t) - y_C(t))^2}{b_1^2} - v_1^2(t) \ge 0, \tag{64b}$$

$$b_{1,H} = \frac{(x_1(t) - x_H(t))^2}{a_1^2} + \frac{(y_1(t) - y_H(t))^2}{b_1^2} - v_1^2(t) \ge 0, \tag{64c}$$

$$b_{U,C} = \frac{(x_U(t) - x_C(t))^2}{a_C^2} + \frac{(y_U(t) - y_C(t))^2}{b_C^2} - v_C^2(t) \ge 0, \tag{64d}$$

Each constraint in (64) ensures that the safe region of CAVs 1 or C is not invaded by surrounding vehicles depicted in Fig. 5. For instance, (64a) necessitates that CAV C maintains a safe distance from the HDV, such that the HDV remains exterior to the defined elliptical safe region.

Optimal Control Problem Formulation. Our goal is to determine the optimal control policy for CAV C to perform a safe lane change maneuver. The objective is to jointly minimize C's energy consumption and speed deviation from traffic flow while guaranteeing safety. Considering cooperations between C and 1, the joint cooperative optimal control problem (OCP) for both CAVs is given by:

$$\begin{aligned} \min_{u_C(t), u_1(t), t_f} & \int_{t_0}^{t_f} \frac{\alpha_u}{2}(u_C^2(t) + u_1^2(t))dt + \alpha_l (y_C(t_f) - l)^2 \\ & + \alpha_v[(v_C(t_f) - v_d)^2 + (v_1(t_f) - v_d)^2] \\ s.t. \; & (60), (61), (62), \end{aligned} \tag{65}$$

where v_d denotes the desired speed of CAVs in the fast lane, $\alpha_u, \alpha_l, \alpha_v$ are adjustable non-negative (properly normalized) weights for energy, desired lateral position, and desired speed, respectively. The CAV dynamics are given in (60) with state and control limits as in (61) and (62). Safety distances between all vehicle pairs in Fig. 5 are constrained through , requiring state knowledge of all vehicles. However, since HDVs are uncontrollable and unknown to CAVs in actuality, coupling the unknown HDV states with CAVs in safety constraints (64a) and (64c) makes (65) directly unsolvable using traditional optimal control methods. The proposed robust control framework can address this problem.

We test our framework by allowing human drivers to manually operate virtual vehicles through a MATLAB interface, and the results show that CAV C can always update its control to avoid collisions and successfully perform a safe maneuver. Our simulation setting is that of Fig. 5. Vehicle U is assumed to travel with constant speed $v_U = 20$ m/s all the time (this is not needed in the overall approach). The allowable speed range for CAVs is $v \in [15, 35]$ m/s, and the acceleration of vehicles is limited to $\boldsymbol{u} \in [(-7, -\pi/4), (3.3, \pi/4)]$ m/s^2. The desired speed v_d for the CAVs is considered as the traffic flow speed, which is set to

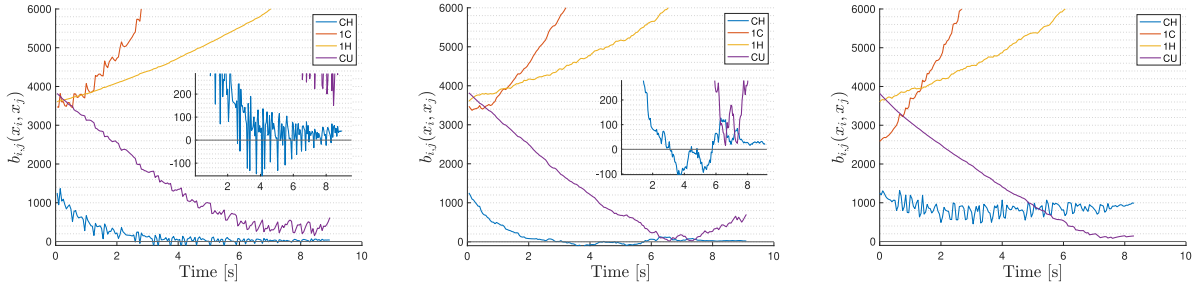

Fig. 7. Safety with time-driven and event-driven CBFs (left to right: time-driven approach with known HDV dynamics, time-driven approach with unknown HDV dynamics, event-driven approach with unknown HDV dynamics). $b_{i,j}(\boldsymbol{x}_i, \boldsymbol{x}_j)$ denotes the value of the CBF between vehicles i and j, where $(i,j) \in \{(C,H),(1,C),(1,H),(C,U)\}$. $b_{i,j}(\boldsymbol{x}_i, \boldsymbol{x}_j) \geq 0$ denotes safety guarantees (Case 3, not Cases 1 and 2).

30 m/s. To guarantee safety, in designing the size of the ellipse in (63) as a safe region, we set the parameters $a_C = a_1 = 0.6$ as the reaction time of CAVs, and $b_1 = b_C = 0.1$ to let the minor axis approximate the lane width $l = 4m$. The maximum allowable maneuver time is set at $T_f = 15s$. The real HDV dynamics are *unknown* to the controller and expressed as:

$$\begin{bmatrix} \dot{x}_H \\ \dot{y}_H \\ \dot{\theta}_H \\ \dot{v}_H \end{bmatrix} = \begin{bmatrix} v_H \cos\theta_H \cdot \sigma_1 \\ v_H \sin\theta_H \cdot \sigma_2 \\ 0 \\ 0 \end{bmatrix} + \begin{bmatrix} 0 & -v_H \sin\theta_H \\ 0 & v_H \cos\theta_H \\ 0 & v_H / L_w \\ 1 & 0 \end{bmatrix} \begin{bmatrix} u_H \\ \phi_H \end{bmatrix} + \begin{bmatrix} \varepsilon_1 \\ \varepsilon_2 \\ \varepsilon_3 \\ \varepsilon_4 \end{bmatrix} \tag{66}$$

where $\boldsymbol{u}_H$ is either a random policy or controlled by a human player. σ_1, σ_2 denote two random processes with uniform pdfs over the interval $[0.9, 1.1]$, and $\varepsilon_1 \in [-0.7, 0.7], \varepsilon_2 \in [-0.5, 0.5], \varepsilon_3 \in [-0.5, 0.5], \varepsilon_4 \in [-0.7, 0.7]$ are disturbances. The initial states of vehicles at time $t_0 = 0$ are given as $\boldsymbol{x}_C(t_0) = [20\text{ m}, 0\text{ m}, 0\text{ rad}, 25\text{ m/s}]^T$, $\boldsymbol{x}_1(t_0) = [50\text{ m}, 4\text{ m}, 0\text{ rad}, 29\text{ m/s}]^T$, $\boldsymbol{x}_H(t_0) = [10\text{ m}, 4\text{ m}, 0\text{ m}, 28\text{ m/s}]^T$, $\boldsymbol{x}_U(t_0) = [60\text{ m}, 0\text{ m}, 0\text{ rad}, 20\text{ m/s}]^T$. The detailed setup using the event-triggered CBF-based QPs is given in Li et al. (2023). The computation times for time-driven and event-driven approaches are 1.5 ms and 24.0 ms, respectively.

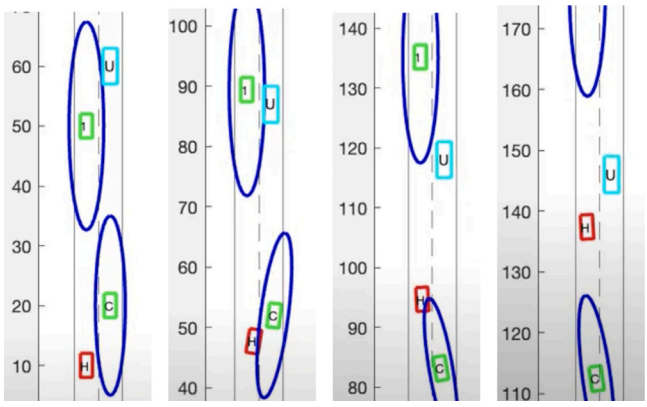

Fig. 8. Snapshots of human study with an aggressive player using the proposed framework (left to right: snapshots t = 0s, t = 1s, t = 3s, t = 5s). The red HDV is controlled by an aggressive human player, the green vehicles are CAVs and the cyan vehicle is a blocking vehicle. Blue ellipses denote safe regions. Safety is guaranteed between the HDV and CAVs with human-in-the-loop. (For interpretation of the references to color in this figure legend, the reader is referred to the web version of this article.)

6.2.1. Comparison between time and event-driven approach

We compare our event-triggered approach in solving CBF-based QPs with unknown HDV dynamics to a time-driven approach. We set the discretized time interval length to be $\Delta = 0.05$ s. Due to inter-sampling effects on system performance when applying a time-driven approach, we consider three cases to test the effectiveness of the event-driven approach in implementing the lane-changing problem. The HDV policy is set to be random, satisfying $u_H(t_k) \in [-1.7, 1.7]\text{ m/s}^2, \phi_H(t_k) \in [-0.2\pi, 0.2\pi]\text{ rad}, k = 0, 1, 2, \ldots$.

Case 1: Time-driven approach with known HDV dynamics. In this case, we assume the HDV dynamics (66) with disturbances are known to CAVs when we apply a time-driven approach.

Case 2: Time-driven approach with unknown HDV dynamics. In this case, the HDV dynamics are unknown to CAVs. Thus, HDV states have to be estimated at each time step $t_k = t_0 + k\Delta$, $k = 0, 1, 2, \ldots$.

Case 3: Event-driven approach with unknown HDV dynamics. Here, we assume HDV dynamics are unknown to CAVs and HDV states have to be estimated at each time step $t_k, k = 0, 1, 2, \ldots$.

The simulation results are shown in Fig. 7, where the x-axis denotes the simulation time and the y-axis denotes the value of safety constraint $b_{i,j}$ in (63). $b_{i,j} < 0$ represents a violation of the safety constraint between vehicles i and j. In Fig. 7, the distances between vehicles 1 and C (red curve), vehicles 1 and H (yellow curve) keep increasing. The two constraints about to be violated are $b_{C,U}$ (purple curve) and $b_{C,H}$ (blue curve). From Fig. 7(a), even if the HDV dynamics are assumed to be known to CAV C, we still have $b_{C,H} < 0$ at some points, which means the distance between vehicles C and H is less than the safe distance. Similar results occur in Fig. 7(b), where $b_{C,H}$ (blue curve) is below 0 at some points, violating safety during the maneuver. Safety is not guaranteed even with state synchronization under the time-driven approach. In Fig. 7(c), all curves are above 0, implying safety guarantees for all vehicles during the lane-changing maneuver.

6.2.2. Human driver case studies

The simulation results in Section 6.2.1 illustrate the effectiveness of the event-driven approach to guarantee safety in lane-changing maneuvers with random HDV policies. We now further introduce human control in the framework, from which the human driver's aggressiveness will affect CAV responses. We have drivers perform *aggressive, hesitant, and conservative* driving behaviors to test the proposed approach through the merging point, safety satisfaction, maneuver time, and energy consumption. The aggressive human driver exhibits accelerator tendencies irrespective of surrounding vehicles, refusing to yield the right-of-way. In contrast, the conservative human driver prioritizes safety contingencies above all else, readily yielding to proximate vehicles. Finally, the hesitant driver is characterized by driving uncertainty, responding to surrounding vehicles with sudden, inconsistent accelerations and decelerations. Taking the aggressive performance as an example, snapshots of how the maneuver evolves are shown in Fig. 8. The simulation results for three types of driving players are summarized in Table 1. Given the safety constraint that is about to be violated is $b_{C,H}$ between vehicles C and H (from the results in Fig. 7), the column "Safety" in Table 1 is defined as the minimum value of $b_{C,H}(t_k), k = 0, 1, 2, \ldots$ during the entire maneuver.

Table 1 shows that if the human driver is aggressive, C is always conservative and chooses to merge behind the HDV. On the contrary,

Table 1
Performance of CAV C under different human driver types. "A-HDV" and "B-HDV" represent merging ahead of HDV and behind HDV, respectively. "Safety" denotes the minimum value of $b_{C,H}$ during the entire maneuver in the repeated 10 times.

Human driver type	Times		Safety	Terminal time t_f [s]	Energy
	A-HDV	B-HDV			
Aggressive	0	10	627.7	3.4 ± 0.3	27.1 ± 25.9
Hesitant	5	5	521.2	8.8 ± 1.4	63.2 ± 46.2
Conservative	10	0	575.6	3.8 ± 0.7	18.8 ± 17.0

if the human driver is conservative, then it is safe for C to behave aggressively and merge ahead of the HDV. If the human driver is hesitant, the merging point varies and depends on the real-time traffic conditions. Note that all values in the Safety column are positive, which indicates no safety constraint is ever violated under the proposed event-driven approach. Moreover, considering the maneuver time t_f in view of energy consumption, we notice that when the driver's intention is explicit, i.e., the human driver is aggressive or conservative, C can respond and merge quickly by adapting to the HDV's behavior: the average maneuver time is $3.4s$ and $3.8s$, respectively, with corresponding energy consumptions 27.1 and 18.8. However, if the human driver performs hesitantly, the driver intention is not clear to CAV C, so that it always travels in a conservative manner with a longer average maneuver time of $8.8s$, and higher energy consumption of 63.2. This motivates exploring an optimal way to evaluate human characteristics in advance so that C can make decisions earlier, hence improving its performance.

7. Future research directions

We have presented an event-triggered framework for safety-critical control of multi-agent systems with unknown dynamics, which enables model-free safety-critical control. This framework is based on defining adaptive affine dynamics to estimate the real system state, and an event-triggering mechanism for solving the problem using a condition we determine that guarantees safety between events. The proposed *model-free* method sets the stage for promising future research along this direction, including:

(1) New relative degree reduction techniques for CBFs to avoid the need for real-time measurements of high order state derivatives. We also need to address the conservativeness of the relative degree reduction methods. We have demonstrated the effectiveness of the proposed framework by applying it to two multi-agent systems with humans in the loop.
(2) Feasibility guarantees for the proposed robust event-triggered CBF method and, more broadly, the CBF method. This infeasibility issue mainly results from the conflict between CBF/HOCBF constraints and control bounds. Although there are preliminary investigations regarding the feasibility of the CBF method (Breeden & Panagou, 2023; Xiao et al., 2022; Xu, Xiao, & Cassandras, 2022), these methods are mostly based on conservative approaches, and it is still challenging to find an effective solution for general constrained optimal control problems.
(3) Safe human interactions. We may explicitly model the dynamics of human controlled agents similar to those of the ego agent. As a result, both the human control and the control of autonomous agent show up in the CBF constraint. Under proper assumptions, it is possible to infer the human control policy using the proposed framework, e.g., in a game-theoretic manner.

Declaration of competing interest

The authors declare that they have no known competing financial interests or personal relationships that could have appeared to influence the work reported in this paper.

Data availability

No data was used for the research described in the article.

References

Ahmad, H., Sabouni, E., Xiao, W., Cassandras, C. G., & Li, W. (2023). Evaluations of cyber attacks on cooperative control of connected and autonomous vehicles at bottleneck points. In *Symposium on vehicles security and privacy (VehicleSec) 2023*.

Ames, A. D., Galloway, K., & Grizzle, J. W. (2012). Control Lyapunov functions and hybrid zero dynamics. In *Proc. of 51rd IEEE conference on decision and control* (pp. 6837–6842).

Ames, A. D., Grizzle, J. W., & Tabuada, P. (2014). Control barrier function based quadratic programs with application to adaptive cruise control. In *Proc. of 53rd IEEE conference on decision and control* (pp. 6271–6278).

Ames, A. D., Xu, X., Grizzle, J. W., & Tabuada, P. (2017). Control barrier function based quadratic programs for safety critical systems. *IEEE Transactions on Automatic Control*, *62*(8), 3861–3876.

Aubin, J. P. (2009). *Viability theory*. Springer.

Borrmann, U., Wang, L., Ames, A. D., & Egerstedt, M. (2015). Control barrier certificates for safe swarm behavior. *IFAC-PapersOnLine*, *48*(27), 68–73.

Boyd, S. P., & Vandenberghe, L. (2004). *Convex optimization*. New York: Cambridge University Press.

Breeden, J., & Panagou, D. (2023). Robust control barrier functions under high relative degree and input constraints for satellite trajectories. *Automatica*, *155*, Article 111109.

Bryson, & Ho (1969). *Applied optimal control*. Waltham, MA: Ginn Blaisdell.

Cheng, R., Khojasteh, M. J., Ames, A. D., & Burdick, J. W. (2020). Safe multi-agent interaction through robust control barrier functions with learned uncertainties. In *Proc. of 59rd IEEE conference on decision and control* (pp. 777–783).

Denardo, E. V. (2003). *Dynamic programming: models and applications*. Dover Publications.

Galloway, K., Sreenath, K., Ames, A. D., & Grizzle, J. (2013). Torque saturation in bipedal robotic walking through control Lyapunov function based quadratic programs. Preprint arXiv:1302.7314.

Glotfelter, P., Cortes, J., & Egerstedt, M. (2017). Nonsmooth barrier functions with applications to multi-robot systems. *IEEE Control Systems Letters*, *1*(2), 310–315.

Khalil, H. K. (2002). *Nonlinea Systems* (3rd ed). Prentice Hall.

Khojasteh, M. J., Dhiman, V., Franceschetti, M., & Atanasov, N. (2020). Probabilistic safety constraints for learned high relative degree system dynamics. In *Proc. of conf. on learning for dynamics and control* (pp. 781–792).

Li, A., Cassandras, C. G., & Xiao, W. (2023). Safe optimal interactions between automated and human-driven vehicles in mixed traffic with event-triggered control barrier functions. arXiv preprint arXiv:2310.00534.

Lindemann, L., & Dimarogonas, D. V. (2019). Control barrier functions for signal temporal logic tasks. *IEEE Control Systems Letters*, *3*(1), 96–101.

Morris, B. J., Powell, M. J., & Ames, A. D. (2015). Continuity and smoothness properties of nonlinear optimization-based feedback controllers. In *2015 54th IEEE conference on decision and control* (pp. 151–158).

Nguyen, Q., & Sreenath, K. (2016). Exponential control barrier functions for enforcing high relative-degree safety-critical constraints. In *Proc. of the American control conference* (pp. 322–328).

Ong, P., & Cortes, J. (2021). Performance-barrier-based event-triggered control with applications to network systems. Preprint arXiv:2108.12702.

Prajna, S., Jadbabaie, A., & Pappas, G. J. (2007). A framework for worst-case and stochastic safety verification using barrier certificates. *IEEE Transactions on Automatic Control*, *52*(8), 1415–1428.

Rawlings, J. B., Mayne, D. Q., & Diehl, M. M. (2018). *Model predictive control: theory, computation, and design*. Nob Hill Publishing.

Sabouni, E., Cassandras, C. G., Xiao, W., & Meskin, N. (2024). Optimal control of connected automated vehicles with event/self-triggered control barrier functions. *Automatica*, *162*, Article 111530.

Sadraddini, S., & Belta, C. (2018). Formal guarantees in data-driven model identification and control synthesis. In *Proc. of the 21st conference on hybrid systems: computation and control* (pp. 147–156).

Tabuada, P. (2007). Event-triggered real-time scheduling of stabilizing control tasks. *IEEE Transactions on Automatic Control*, *52*(9), 1680–1685.

Tan, X., Shaw Cortez, W., & Dimarogonas, D. V. (2021). High-order barrier functions: Robustness, safety and performance-critical control. *IEEE Transactions on Automatic Control*, 1.

Taylor, A. J., Ong, P., Cortes, J., & Ames, A. D. (2021). Safety-critical event triggered control via input-to-state safe barrier functions. *IEEE Control Systems Letters*, *5*(3), 749–754.

Taylor, A. J., Singletary, A., Yue, Y., & Ames, A. D. (2020). Learning for safety-critical control with control barrier functions. In *Proc. of conf. on learning for dynamics and control* (pp. 708–717).

Tee, K. P., Ge, S. S., & Tay, E. H. (2009). Barrier Lyapunov functions for the control of output-constrained nonlinear systems. *Automatica*, *45*(4), 918–927.

Wieland, P., & Allgower, F. (2007). Constructive safety using control barrier functions. In *Proc. of 7th IFAC symposium on nonlinear control system*.

Wisniewski, R., & Sloth, C. (2013). Converse barrier certificate theorem. In *Proc. of 52nd IEEE conference on decision and control* (pp. 4713–4718). Florence, Italy.

Xiao, W., & Belta, C. (2019). Control barrier functions for systems with high relative degree. In *Proc. of 58th IEEE conference on decision and control* (pp. 474–479). Nice, France.

Xiao, W., Belta, C., & Cassandras, C. G. (2021a). Adaptive control barrier functions. *IEEE Transactions on Automatic Control*, *67*(5), 2267–2281.

Xiao, W., Belta, C., & Cassandras, C. G. (2021b). High order control Lyapunov-barrier functions for temporal logic specifications. In *Proc. of the American control conference* (pp. 4886–4891).

Xiao, W., Belta, C., & Cassandras, C. G. (2022). Sufficient conditions for feasibility of optimal control problems using control barrier functions. *Automatica*, *135*, Article 109960.

Xiao, W., Belta, C., & Cassandras, C. G. (2023). Event-triggered control for safety-critical systems with unknown dynamics. *IEEE Transactions on Automatic Control*, *68*(7), 4143–4158. http://dx.doi.org/10.1109/TAC.2022.3202088.

Xiao, W., & Cassandras, C. G. (2021). Decentralized optimal merging control for connected and automated vehicles with safety constraint guarantees. *Automatica*, 123.109333.

Xiao, W., Cassandras, C. G., & Belta, C. (2023). *Safe autonomy with control barrier functions: theory and applications*. Springer Nature.

Xu, K., Xiao, W., & Cassandras, C. G. (2022). Feasibility guaranteed traffic merging control using control barrier functions. In *2022 American control conference* (pp. 2309–2314). IEEE.

Yang, G., Belta, C., & Tron, R. (2019). Self-triggered control for safety critical systems using control barrier functions. In *Proc. of the American control conference* (pp. 4454–4459).